Guo *et al. Microstructures* 2023;3:2023038
DOI: 10.20517/microstructures.2023.30

Microstructures

Review

Open Access

Check for updates

The concept, structure, and progress of seawater metal-air batteries

Yuanyuan Guo[1], Yanhui Cao[2], Junda Lu[1], Xuerong Zheng[1,2], Yida Deng[1,2]

[1]State Key Laboratory of Marine Resource Utilization in the South China Sea, School of Materials Science and Engineering, Hainan University, Haikou 570228, Hainan, China.
[2]School of Materials Science and Engineering, Key Laboratory of Advanced Ceramics and Machining Technology of Ministry of Education, Tianjin University, Tianjin 300072, China.

Correspondence to: Prof. Xuerong Zheng, State Key Laboratory of Marine Resource Utilization in South China Sea, School of Materials Science and Engineering, Hainan University, Haikou 570228, Hainan, China. E-mail: xrzh@hainanu.edu.cn; Prof. Yida Deng, State Key Laboratory of Marine Resource Utilization in the South China Sea, School of Materials Science and Engineering, Hainan University, Haikou 570228, Hainan, China. E-mail: yd_deng@hainanu.edu.cn

How to cite this article: Guo Y, Cao Y, Lu J, Zheng X, Deng Y. The concept, structure, and progress of seawater metal-air batteries. *Microstructures* 2023;3:2023038. https://dx.doi.org/10.20517/microstructures.2023.30

Received: 5 Jun 2023 **First Decision:** 29 Jun 2023 **Revised:** 16 Jul 2023 **Accepted:** 31 Jul 2023 **Published:** 10 Oct 2023

Academic Editor: Zaiping Guo **Copy Editor:** Fangyuan Liu **Production Editor:** Fangyuan Liu

Abstract

Seawater metal-air batteries (SMABs) are promising energy storage technologies for their advantages of high energy density, intrinsic safety, and low cost. However, the presence of such chloride ions complex components in seawater inevitably has complex effects on the air electrode process, including oxygen reduction and oxygen evolution reactions (ORR and OER), which requires the development of highly-active chloride-resistant electrocatalysts. In this review, we first summarized the developing status of various types of SMABs, explaining their working principle and comparing the battery performance. Then, the reported chlorine-resistant electrocatalysts were classified. The composition and structural design strategies of high-efficient chlorine-resistant ORR/OER electrocatalysts in seawater electrolytes were comprehensively summarized. Finally, the main challenges to be overcome in the commercialization of SMABs were discussed.

Keywords: Seawater metal-air batteries, oxygen reduction reactions, oxygen evolution reactions, chloride-resistant

INTRODUCTION

Renewable energy resources, such as wind energy, solar energy, and wave energy, exist extensively,

especially on the sea[1,2]. Harvesting energy directly from the sea provides great potential for developing the marine economy and promoting marine research. Thus, developing renewable energy utilization techniques, such as wind power generation, photovoltaics, and hydroelectric generation, is highly demanded for providing green electricity to the marine equipment[3-5]. However, the intermittent power supply property makes the clean energy sources difficult to be utilized efficiently. Moreover, traditional secondary batteries, such as Lithium (Li)-ion batteries and Lead-acid batteries, cannot meet the long-term and high-power density requirements of the equipment working in the deep and open sea[6,7]. Therefore, harvesting energy directly from the ocean is critically demanded.

Seawater metal-air batteries (SMABs) are considered as extremely promising power sources for providing electricity for the equipment working on the sea or in the deep sea due to their high theoretical energy density, low cost, eco-friendly nature, *etc.*[8,9]. During the discharge of SMABs, seawater is directly used as the electrolyte, the dissolved oxygen (O_2) in seawater is reduced on the cathode, and the metallic anode [Magnesium (Mg), Aluminum (Al), Sodium (Na), *etc.*] is oxidized[10,11]. The working processes are summarized as follows:

$$\text{Cathode:} \quad O_2 + 2\,H_2O + 4\,e^- \rightarrow 4\,OH^- \tag{1-1}$$

$$\text{Anode:} \quad M \rightarrow M^{n+} + n\,e^- \tag{1-2}$$

$$\text{Total reaction:} \quad 4\,M + n\,O_2 + 2n\,H_2O \rightarrow 4\,M(OH)_n \tag{1-3}$$

The dissolved O_2 was harvested from seawater and subsequently reduced through the oxygen reduction reaction (ORR), while the metals (alloys) were oxidized, forming metallic hydroxides[12,13]. Due to the open structure of SMABs, oxygen, as an active species, can infinitely diffuse to the cathode for ORR, which ensures the SMABs display high theoretical energy density[14,15]. One critical issue is that the un-optimized electronic structure of metallic sites and the four reaction steps for the ORR process would result in sluggish catalytic kinetics[16]. Although the OER is thermodynamically favored over the hypochlorite formation reaction in seawater (pH ≈ 8), both reactions were a balancing relationship during seawater catalysis owing to the slow catalytic kinetics in seawater[17,18]. Currently, we consider OER to be the primary cathode reaction upon the charging of seawater batteries. Thus, designing and exploring efficient and low-cost electrocatalysts is an urgent task to enhance the battery performance. In the past few years, various types of electrocatalysts were designed to accelerate the ORR/OER catalytic kinetics in seawater, including noble metals of Pt, Ru, Ir, and their alloys[19-21]. However, the noble metals are more easily being poisoned in seawater electrolytes. The non-noble metal electrocatalysts, such as Fe groups (Fe, Co, Ni) and carbon-based materials with abundant and inexpensive advantages, have been explored, displaying satisfying ORR performance and deserving further exploration as promising ORR/OER electrocatalysts in seawater conditions[22-24]. At the same time, the circulating seawater electrolyte can promote the heat and charge transfer rate, thereby improving the intrinsic safety and cycle life of the SMABs[25,26]. Therefore, the SMABs are particularly suitable as long-term power supply systems for the equipment working in the sea.

However, in comparison to the alkaline metal-air battery systems, the high content of chloride ions (Cl^-) in seawater (19.345 g/kg) is easily absorbed on the surface of electrocatalysts. This absorption changes the electronic structure and poisons the metallic sites, thereby greatly reducing the power density of SMABs[27,28]. Although some electrocatalysts display good ORR catalytic performance in conventional electrolytes, they cannot maintain active and stable in seawater electrolytes due to the poison of high concentration of Cl^-[29]. The recent results suggest that, on the one hand, the adsorption of Cl^- on the surface catalytic sites can hinder the breakage of O-O bonds and thus inducing the reaction pathway change from a four-electron to a sluggish two-electron pathway for the ORR process[30,31]. Moreover, the adsorption of O_2 molecules would also be suppressed. On the other hand, due to competitive chlorine evolution reaction

(ClER) and chloride corrosion, the oxygen evolution reaction (OER) performance of the catalysts in seawater electrolytes decays rapidly during charging[32]. Therefore, it remains a great challenge for the development of efficient chlorine-resistant ORR/OER electrocatalysts for their application in seawater electrolytes for SMABs.

In order to put forward the wide application of SMABs in the field of marine techniques, three key issues need to be solved urgently: (i) The poisoning mechanism of Cl^- on ORR/OER processes in seawater electrolytes should be clarified, thus providing guidance for designing high-efficient chlorine-resistant catalysts; (ii) The electronic structure of noble metal catalysts should be optimized to enhance the electrocatalytic activity and stability in seawater electrolytes. Specifically, this can be achieved through several strategies. Firstly, by modifying the ligands or surface modifiers, the electronic structure of the catalyst can be adjusted. This influences the distribution of electron density and the reactivity of the active sites, leading to improved electrocatalytic performance. Secondly, introducing suitable elements into the noble metal catalyst can modify its electronic structure. This alters the binding strength of reactants and intermediates, facilitating the desired electrochemical reactions and enhancing catalytic activity and stability. Thirdly, modifying the surface of the catalyst through techniques such as surface deposition or functionalization can regulate its electronic structure. This can enhance the interaction with reactants and ions in the electrolyte, improving catalytic activity and stability. At the same time, chlorine-resistant non-noble metal-based electrocatalysts with excellent ORR/OER performance should be developed to broaden the types of catalysts and reduce the cost of catalysts; and (iii) The integrated structure of SMABs should be optimized to improve the power density and stability of batteries. Based on the above consideration, this review presents the progress in the development of chlorine-resistant cathode electrocatalysts for SMABs. In this review, we first summarized the development of various types of SMABs to understand their working principle and battery performance [Figure 1]. Subsequently, the poisoning mechanism of Cl^- on cathode electrocatalysts during charging and discharging was studied and summarized. Then, we classified the reported chlorine-resistant electrocatalysts and comprehensively summarized the composition and structural designing strategies of high-efficient chlorine-resistant ORR/OER electrocatalysts in seawater electrolytes. Finally, the main challenges to be addressed in the commercialization of SMABs were discussed.

THE DEVELOPING HISTORY OF SEAWATER METAL-AIR BATTERIES

The SMABs were developed through three stages, starting from seawater-activated batteries (SABs) to primary SMABs (P-SMABs). and further evolving into rechargeable SMABs (R-SMABs)[33]. The SAB was originally developed in the 1940s by Bell Telephone Laboratories to meet the requirement for high energy density, prolonged shelf-life, and outstanding low temperature performance. It was mainly used as a power source for military torpedoes. The SAB, which used magnesium as the anode, silver chloride (AgCl) as the cathode, and flowing seawater as the electrolyte, was first commercialized in 1943, as shown in Figure 2A. The battery can be stored for up to five years in a dry condition and can be activated by the addition of seawater when being used, thus being called SAB. During the discharge, the following reactions occur[34]:

$$\text{Anodic reaction:} \quad Mg - 2e^- \rightarrow Mg^{2+} \tag{2-1}$$

$$\text{Cathodic reaction:} \quad AgCl + e^- \rightarrow Ag + Cl^- \tag{2-2}$$

The above reaction possesses fast catalytic kinetics. For discharging, the AgCl on the cathode of the battery is reduced to Ag, leading to an increase in conductivity as the process proceeds. However, the discharge voltage would drop dramatically when AgCl is reduced to Ag completely. Moreover, another advantage of the Mg-AgCl battery system is that the device can keep working efficiently in wide temperature ranges. The

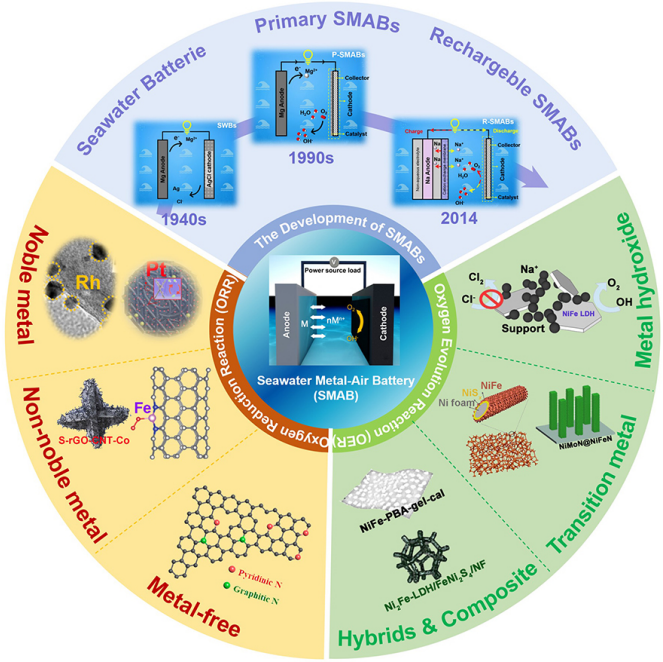

Figure 1. Schematic diagram of the classification of SMABs and ORR/OER electrocatalysts. (Reproduced with permission[91]. Copyright 2021, Elsevier; Reproduced with permission[92]. Copyright 2011, Wiley-VCH; Reproduced with permission[97]. Copyright 2017, Elsevier; Reproduced with permission[99]. Copyright 2021, Wiley-VCH; Reproduced with permission[104]. Copyright 2020, American Chemical Society; Reproduced with permission[128]. Copyright 2022, WILEY-VCH; Reproduced with permission[127]. Copyright 2022, WILEY-VCH; Reproduced with permission[121]. Copyright 2019, PNAS; Reproduced with permission[120]. Copyright 2019, Springer Nature; Reproduced with permission[114]. Copyright 2016, Wiley-VCH).

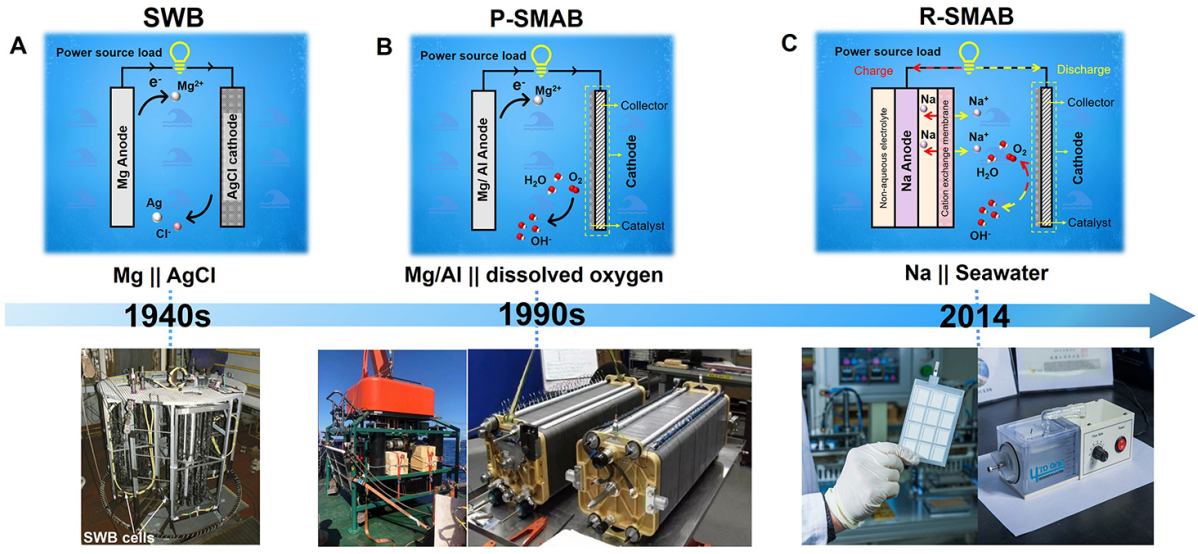

Figure 2. Timeline of the development of seawater-based batteries from SWBs to rechargeable SMABs.

discharge voltage can remain stable when the temperature changes from 219 K to 369 K, and the output power density has no obvious change. Therefore, the SAB generally displays remarkable advantages of steady discharge voltages, high discharge current densities, and high output powers of up to 70 kW. Up to now, the maximum discharge current density and voltage of SABs reached 2 A cm^{-2} at about 1.32 V.

However, due to the large amount of consumption of precious silver and the resulting high cost, the SAB was only being used in the military area. Recently, many efforts have been devoted to reducing the battery manufacturing cost and to further increase the total power. For instance, a variety of Mg, Al, zinc (Zn), and Na alloys have been explored for being used as the anodes[35-48], while the cuprous chloride[34], cuprous iodide[49,50], lead chloride[51] and mercurous chloride[52] have been explored as the cathodes of SABs. However, up to now, none of these systems can completely replace the Mg/AgCl system.

In the 1990s, the primary metal-air batteries driven by dissolved O_2 in seawater attracted attention due to their high theoretical energy density. The devices of P-SMABs mainly use Zn, Mg, and Al as anodes. The cathodic and anode electrochemical reactions for P-SMABs are as follows[53]:

$$\text{Cathodic reaction:} \quad O_2 + 2H_2O + 4e^- \rightarrow 4OH^- \tag{2-3}$$

$$\text{Anode reaction:} \quad M \rightarrow M^{n+} + ne^- \tag{2-4}$$

However, due to the slight solubility of oxygen in seawater, the battery performance is limited by the oxygen concentration and diffusion, thus leading to relatively low current density and operating voltage (1.0 V to 1.8 V). The P-SMABs, as a type of semi-fuel cells, have attracted tremendous attention due to their environmental friendliness and low cost. The geometrical structure of P-SMABs is similar to that of SABs. The key difference lies in the cathode materials and the related reduction reaction that occurred on cathodes.

The electrocatalysts on the cathode, such as graphite electrodes and carbonized fibers, play a critical role in accelerating ORR processes, as shown in Figure 2B. The unsatisfying battery performance of P-SMABs makes it difficult to meet the requirements of underwater equipment for high power density, and thus, most P-SMABs are mainly being used in some long-endurance, low-power underwater equipment[53-55]. Recently, Shinohara *et al.* installed a seafloor borehole broadband seismic observatory in the northwestern Pacific basin, where the water depth is 5,577 m[54]. The observatory is powered by a system of four P-SMAB systems connected in series. The battery system can effectively power the monitoring system (the average power consumption is 6 W) and the Data Logger for at least five years. To enhance the current density and power density, one strategy is to develop efficient electrocatalysts with exposure to large active sites and higher intrinsic catalytic kinetics. This accelerates the ORR process while ensuring robust chlorine-corrosion resistance in natural seawater electrolytes.

To endow seawater batteries with the capability of storing electrical energy, Hwang *et al.* proposed and patented R-SMABs with half-opening structures in 2014[33]. In this system, seawater not only serves as an electrolyte and provides the reactant for the cathode but also as a supplier of anode material. In the R-SMABs, sodium was used as the anode, electrocatalysts connected to the current collector as the cathode, and solid-state electrolytes as channels for transporting sodium ions and flowing seawater, as shown in Figure 2C. During the charging process of R-SMABs, the anodes capture sodium ions from seawater in non-aqueous anolytes, while the cathode undergoes OER. During the discharging process, the sodium in the anode dissolves into sodium ions and is transferred to seawater, and the cathode reacts in the same way as the P-SMABs [Equations 5 and 6]. The half-cell reaction equations of the charging and discharging processes for R-SMABs are listed as follows[51]:

$$\text{Anode reaction:} \quad 4Na^+ + 4e^- \leftrightarrow 4Na \tag{2-5}$$

$$\text{Cathodic reaction:} \quad 4OH^- \leftrightarrow O_2 + 2H_2O + 4e^- \ (\text{ORR}\leftrightarrow\text{OER}) \tag{2-6}$$

The theoretical voltage of the R-SMABs can reach 3.48 V. However, due to the sluggish catalytic kinetics of electrocatalysts in cathodes, the Cl^- corrosion on both cathodes and anodes, and the competing relationship between the two electrodes, the battery system is still far from reaching its theoretical properties[56-60]. To put forward the practical application of SMABs, such as the typical sodium-based seawater batteries, the power density, capacity, and stability of the SMABs should be further optimized. The SMABs can be divided into small (< 1 kWh), medium (1-10 kWh), and large-scale (> 1 MWh) power sources according to their discharging capacity. Some low-power seawater-based metal-air battery prototypes have been utilized for underwater observation and ocean buoys. Medium-power seawater batteries can be used for exploratory unmanned aerial vehicles and maritime search and rescue operations. The stability of large-scale seawater batteries should be further optimized for their large-scale application in the future.

THE COMPONENTS AND EVALUATION OF SEAWATER METAL-AIR BATTERY

The large-scale commercialization of efficient and stable SMABs remains a significant challenge, which requires the optimization of all individual components in the battery. As discussed above, SMABs feature an open structure. The essential components in the battery contain electrode materials (cathodes and anodes), electrolytes (anolytes, catholytes), current collectors, ceramic solid electrolytes, electrocatalysts, and the general cell type, depending on different categories of SMABs.

Electrocatalysts and electrode materials

SMABs are basically composed of anodes and cathodes with current collectors. The electrocatalysts were mixed with binders and were pasted onto the current collectors for preparing electrodes[61,62]. Highly efficient SMABs require electrodes (both anodes and cathodes) with optimized electronic conductivity, porous density, and wettability[63,64]. The electrodes should meet several prerequisites for developing efficient and stable SMAB devices [Figure 3A]. Developing anode materials should meet the following requirements: (i) avoid the side reactions that may lead to cell swelling and failure; (ii) possess good electronic conductivity and excellent stability in seawater conditions; and (iii) narrow voltage window, low-cost and low toxicity. At present, SMABs with anodes consisting of Li, Na, Mg, Al, Zn, and their alloys have been systematically studied[65,66]. Among various types of SMABs, seawater lithium-air batteries theoretically possess the highest energy density, reaching up to 11,140 $Wh{\cdot}kg^{-1}$. On the other hand, metals such as Zn, Mg, and Al display the advantages of environmental friendliness, abundance in the Earth's crust, low cost, and intrinsic safety. In addition, Al is readily available for recycling in massive amounts and has a high energy density of 8,100 $Wh{\cdot}kg^{-1}$ and a significant theoretical voltage of 2.7 V[67]. As a result, seawater aluminum-air batteries are considered as the most promising systems for developing SMABs.

The air cathode is composed of a gas diffusion layer (GDL), electrocatalyst, and current collector. As mentioned above, the OER and ORR occur in the cathodes when seawater batteries are charged and discharged, respectively[68]. Therefore, an efficient air electrode should possess strong oxygen adsorption capacity, fast oxygen diffusion, and high electrochemical activity for oxygen redox reactions in SMABs. The electrocatalyst layer in the cathode has a significant influence on the performance of SMABs. The electrocatalysts on the cathodes may be noble metals, transition metals (TM), and non-metallic materials. Moreover, the electrocatalysts should not only display efficient ORR and OER activity and stability but also possess strong Cl^- corrosion resistance with stable physical structures in seawater conditions. The Cl^- in seawater can easily destroy the oxide thin film on the surface of the electrocatalysts and form complexes with metal ions, resulting in corrosion of metallic sites in seawater[53,69]. The electrocatalysts can be divided into the following three categories: (1) noble metals and their alloys, such as Pt as ORR electrocatalysts while IrO_x and RuO_x as OER electrocatalysts; (2) non-noble metal-based catalysts, such as metal-supported carbon materials and metal oxides and sulfides; and (3) metal-free electrocatalysts, such as nitrogen (N) doping

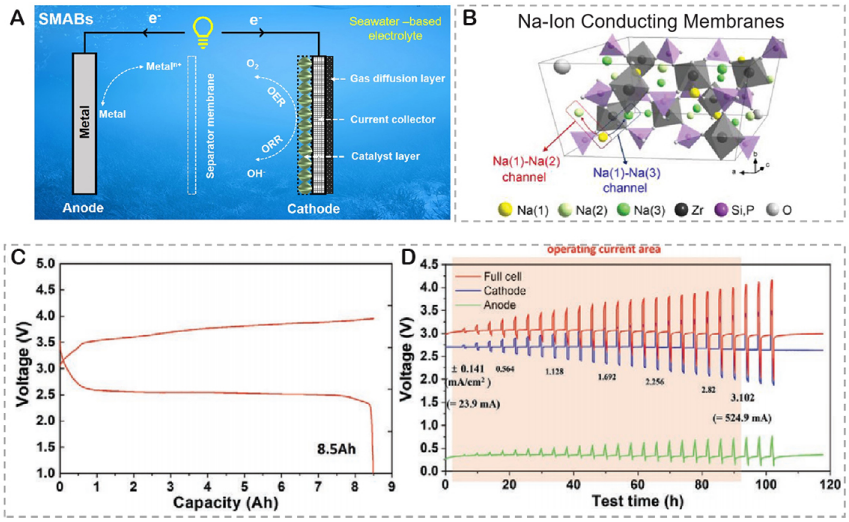

Figure 3. (A) a schematic illustration of the basic components. (B) Schematic of monoclinic structures of Na-Ion Conducting Membranes (Solid Electrolytes). (Reproduced with permission[33]. Copyright 2018, Wiley-VCH) Parameters of performance evaluation. (C) Capacity and (D) efficiency. (Reproduced with permission[61]. Copyright 2022, Wiley-VCH).

carbon. Currently, carbon-based functional materials have been recognized as promising electrocatalysts for their high corrosion resistance and are thus being utilized in the SMAB[70,71]. Generally, carbon-based materials can be divided into carbon cloth, conductive carbon paper, and graphitic fiber. The GDL undertakes multiple tasks in the electrodes. It acts as a connector between the air and the catalyst, allowing oxygen to diffuse from the air atmosphere to the surface and further to the inner of an electrode, or in other words, it absorbs oxygen from the surrounding environment for OER and ORR catalysis. The GDL in the cathodes should have the following characteristics: hydrophobicity, lightness, thinness, and high porosity. It is often composed of electrocatalysts and hydrophobic binders, such as polytetrafluoroethylene (PTFE)[72].

Electrolyte

SMABs are chemical power sources with seawater as electrolytes. Seawater is a naturally available, abundant, and renewable resource, accounting for about 70% of the Earth's surface. According to the seawater data, the salt content per liter of water reaches about 35 g. In addition to the main components of sodium chloride (NaCl), there are many other cations and anions in seawater, such as calcium, magnesium, sulfates, bicarbonates, and fluorides[53,73]. The dissolved salt ions in seawater contribute to its high ionic conductivity of about 50 mS cm^{-1} (at 20 °C). Therefore, seawater is considered as the electrolyte for electrochemical cells. Furthermore, seawater contains not only dissolved salt ions but also dissolved gases, such as oxygen, which can act as cathode-oxidants to react with H_2O molecules on cathode current collectors. However, the composition of seawater varies based on factors such as location, depth, time, climate, and environmental conditions.

Natural seawater contains abundant calcium ions and impurities, which can lead to calcium deposits and deactivation of the active materials, thus hindering effective contact between the electrode and electrolyte. In addition, the impurities in seawater may undergo side reactions with the anode and cathode, resulting in performance degradation or irreversible damage to the battery. To avoid the impurity ions in natural seawater, the simulated seawater and artificial seawater were also employed as electrolytes for the rechargeable metal-air batteries. The simulated and artificial seawater typically contains the following components: (i) salts such as NaCl, magnesium sulfate ($MgSO_4$), calcium sulfate ($CaSO_4$), *etc.*; (ii) pH adjusters such as sodium hydroxide (NaOH) or sulfuric acid (H_2SO_4) to adjust the pH value of the electrolyte; and (iii) dissolved organic compounds and trace elements, such as dissolved O_2, silicates, iron,

manganese, *etc.* The specific composition and ratio of the simulated seawater electrolyte can be adjusted and optimized according to the specific research purposes and experimental requirements. In addition, the organic electrolytes containing NaCl were also being developed for their application in R-SMABs. This is because the organic electrolyte possesses good ion conductivity and fewer side reactions for charging and discharging. Commonly used organic electrolytes include ethylene glycol dimethyl ether (EGDME), acrylonitrile (AN), and propylene glycol (PG), which have good solubility and high ion conductivity.

Current collector

Although there is no solid electrode in this battery system, a current collector is still needed. It facilitates the transport of electrons released from the anode part during the deintercalation/dealloying process. Moreover, the current collector carries cathodic reactions (OER and ORR), which are necessary for related charge transport. Compared to the typical organic batteries with solid cathodes, current collectors usually require special properties, such as stability in saltwater[74].

In the cathode chamber, the role of the current collector is to support the active materials and collect and transfer the electrons to the external circuit. In order to effectively promote the sluggish oxygen reaction kinetics, the current collector on the cathode should possess the advantages of high electronic conductivity, good electrochemical and mechanical stability, and large specific surface area.

In the anode chamber, the current collector should remain stable and work well with the anode materials (such as Mg, Al, and their alloys) and the electrolytes in the batteries. During working, the current collector should ensure the electrons transfer stably from electrolytes to the anode active materials. The commonly used current collectors are generally porous metal foams, such as nickel foam, copper foil, stainless steel, *etc.* Recently, newly developed carbon-based collectors are commonly used in seawater batteries, which could not only offer catalytic sites for the ORR and OER processes but also ensure an efficient charge transferring rate[74,75].

Separator membrane

Sodium-ion-conducting membranes are widely used as separators to separate the anode and cathode compartments in R-SMABs [Figure 3B][33,76]. Such membrane materials are commonly used as solid electrolytes in solid-state batteries. The stability of the membrane in different types of liquid electrolytes should be stable to ensure the stability of the entire battery in both organic and aqueous solutions, especially for some SMABs that should work under high current density and voltage conditions. Therefore, the separator membrane should remain stable in a relatively wide electrochemical potential window to keep the battery working for long-term utilization. In addition, the solid electrolyte as the separator for seawater batteries also needs to have high sodium ion conductivity, good mechanical properties, and ultra-low porosity to avoid electrolyte penetration.

Criteria for evaluating the seawater metal-air battery performance

The SMABs should be assembled into a package before testing, and they generally contain three parts: an organic anode chamber, a seawater cathode chamber, and a separator. These three parts were sealed to avoid the electrolyte linkage. The distance between an anode, cathode, and separator should be kept constant to evaluate the performance of different SMABs. To evaluate the battery performance, the open circuit voltage, discharging capacity, power density, and other indexes were systematically tested. Typically, the capacity is one of the most important performance indexes to measure seawater battery performance, which describes the charge storage capacity of the SMAB (the amount of charge Q that a battery can provide or store) [Figure 3C], usually expressed as ampere-hour (Ah) and normalized to mass (Ah g^{-1}) or volume (Ah cm^{-3}). The value of battery capacity can be influenced by the discharge rate, discharge current,

discharge voltage, temperature, geometry dimension of the anode and cathode, and the mass loading of active materials[77]. Generally, it is difficult to reach the theoretical capacity in practical applications due to the polarization effects and the side reactions during charging and discharging. Therefore, increasing the capacity of seawater batteries requires not only performance improvement of cathode/anode materials but also the optimization of the structure of the whole device.

Coulombic and energy efficiencies are typical parameters in electrochemical systems of R-SMABs, which represent the ratio of the amount of charge (Q) flowing through the battery and the voltage ratio between charging and discharging, respectively [Figure 3D]. A coulomb efficiency is usually used as a comparative value to determine the capacity loss for each cycle in the rechargeable battery systems, which is an important parameter to predict the remaining life of the battery[78,79]. However, the performance of coulombic and energy efficiencies can be influenced by many factors, such as the environmental temperature, the humidity, and the uniformity of each package and electrode. Therefore, to precisely evaluate the key factors and the mechanisms that influence enhanced battery performance, the standard experimental procedure should be established.

Stability and safety are key parameters in assessing the performance of SMABs. The stability of positive electrodes in the seawater medium is one of the biggest factors for determining the long-term performance of the whole battery[61]. Due to the existence of Cl^- in seawater electrolytes, more surface metallic sites would be attacked, thus decreasing the exposure of metallic sites. Moreover, the Cl^- adsorption would change the reaction pathway. For instance, the ORR pathway would be transferred from $4e^-$ in alkaline electrolytes to $2e^-$ in seawater electrolytes[80]. As a result, it is a critical challenge to develop Cl^- corrosion-resistant electrocatalysts to enhance the stability of cathodes and the whole SMAB devices. Moreover, because seawater was employed as the electrolyte without the use of any organic additives, the SMABs possess highly intrinsic safety and are eco-friendly[81-83]. In addition, the seawater battery is a semi-open or fully open electrochemical system, which is beneficial for gas release and temperature diffusion, thus keeping the system working in relatively low temperature conditions (generally lower than 60 °C).

ORR ELECTROCATALYSTS IN SEAWATER ELECTROLYTE

The oxygen electrocatalytic process in seawater is considered as a complicated pathway, which may involve the simultaneous occurrence of oxygen reduction and chlorine corrosion, depending on the condition of pH values, oxygen/chlorine concentration, temperature, *etc.*[83-85]. The absorption and corrosion of Cl^- play a critical role in enhancing the catalytic efficiency and stability of the catalysts, thus affecting the battery performance. In this section, we discussed the development of ORR electrocatalysts and the influence behavior of Cl^- toward the ORR process[86].

ORR mechanism and Cl^--resistance mechanism in seawater batteries

The ORR mechanism in seawater involves the reduction of dissolved O_2 by a four-electron process to hydroxide ions (OH^-) or by a two-electron process to form hydrogen peroxide (H_2O_2) on the cathode electrocatalysts. In the four-electron process, each oxygen molecule (O_2) accepts four electrons and undergoes a complete reduction to form OH^-. This is the most favorable pathway for ORR as it does not produce any intermediate reactive species. The reaction process can be represented as follows:

$$O_2^* + e^- + H_2O \rightarrow OOH^* + OH^- \quad (4\text{-}1)$$

$$OOH^* + e^- \rightarrow O^* + OH^- \quad (4\text{-}2)$$

$$O^* + e^- + H_2O \rightarrow OH^* + OH^- \quad (4\text{-}3)$$

$$OH^* + e^- \rightarrow OH^- \quad (4\text{-}4)$$

In the two-electron process, each dissolved O_2 molecule accepts only two electrons, resulting in the formation of H_2O_2. This pathway is less desirable as it can lead to the generation of reactive oxygen species and undesirable byproducts. The overall reaction can be represented as follows:

$$O_2^* + e^- + H_2O \rightarrow OOH^* + OH^- \quad (4\text{-}5)$$

$$OOH^* + e^- + H2O \rightarrow H_2O_2 + OH^- \quad (4\text{-}6)$$

Cl^- is among the most abundant ions in seawater electrolytes. However, due to the specific Cl^- blocking effect, the Cl^- tends to adsorb on the surface catalytic sites of the cathodes. The adsorption of Cl^- would cause several serious results: (1) the active site exposure would be reduced, thus causing the decrease of ORR current density; (2) the electronic structure of surface metallic sites would be changed, thus causing the poison of catalytic sites[52,86]; and (3) the local bonding environment of active sites would be tuned in the catalysts and cause the dissolution of metal atoms, thus worsening the stability of cathodes. Currently, the reversibility of Cl^- adsorption is still debatable. Along with the blocking effect, Cl^- adsorption behavior would affect the breakage of O-O bonds during ORR processes, thus changing the ORR pathway from a four-electron to a two-electron mechanism, leading to the generation of H_2O_2. More importantly, the existence of H_2O_2 at the three-phase interface (gas-solution-solid) will produce free radicals that can attack the metal anodes or/and electrocatalysts, thus resulting in the reduction of durability[87,88]. In order to overcome the bad influence of Cl^- on the catalytic process in seawater, the ORR electrocatalyst generally should possess the prerequisites of high electronic conductivity and electrochemical stability in saltwater electrolytes. In addition, other criteria such as large specific surface area, high intrinsic catalytic activity, and low mass loading are also should be considered[88]. Based on the related reports, ORR electrocatalysts can be classified into three categories: noble metal-based materials, non-noble metal-based electrocatalysts, and metal-free electrocatalysts. This section will summarize the research efforts that have focused on enhancing the catalytic performance of different electrocatalysts in SMABs.

Noble metal-based ORR electrocatalysts

Noble metal-based ORR electrocatalysts, especially Pt-based catalysts, usually have high ORR efficiency, but they are expensive and can be easily destroyed by a large amount of Cl^- in seawater. Besides, the formation of soluble chlorine complexes (such as $PtCl_4^{2-}$) can also lead to the dissolution of platinum and the surface passivation of metallic sites, which adversely affects the stability of ORR[89,90]. Recently, Ryu *et al.* designed a Pt-Co alloy electrocatalyst using carbothermal shock (CTS) for use in high-performance seawater batteries[91]. The authors prepared single and blended aqueous solutions of $H_2PtCl_6 \cdot 6H_2O$ and $CoCl_2$ precursors with different ratios to synthesize the Pt-Co alloy on heated carbon felt (HCF) within 10 s [Figure 4A and B]. Figure 4C enabled us to observe that the peak at q = 2.77 A^{-1} shifted to a higher value, indicating that the formation of Pt-Co alloy leads to lattice contraction. Moreover, the Pt 4f XPS spectra of the samples mentioned above show that the peaks of Pt $4f_{5/2}$ and Pt $4f_{7/2}$ shift to high binding energy, mainly due to the loss of 5d electrons in Pt-based alloys, indicating the formation of Pt-Co alloys. As shown in Figure 4D, the catalyst with Pt:Co = 2:1 achieved high current density and low overpotential in the ORR process for the synergistic effect between the Pt and Co metallic sites. Moreover, the Pt-Co alloy electrocatalyst can remain stable in the seawater catholyte, and thus, the seawater batteries using Pt-Co alloys as cathodes exhibit excellent cycling stability with no obvious degradation [Figure 4E]. Compared to the SMAB using pristine HCF as a current collector, the battery using a composition of Pt-Co nanoparticle (NP)-decorated CF can be cycled at 0.3 mA cm^{-2} for up to 500 h without substantial performance deterioration. In addition, Jin et a*l.* reported well-dispersed $Rh_{17}S_{15}$ NPs supported on carbon nanotube (CNT) substrates[92]. The diameter of the embedded particles was evenly about 8 nm, and the mass loading of Rh reaches 25 wt% when pyrolyzed at 650 °C. The ORR catalytic activity of the nanocomposites is highly active under Cl^- electrolysis conditions, which could exhibit considerable stability in the chloride environment.

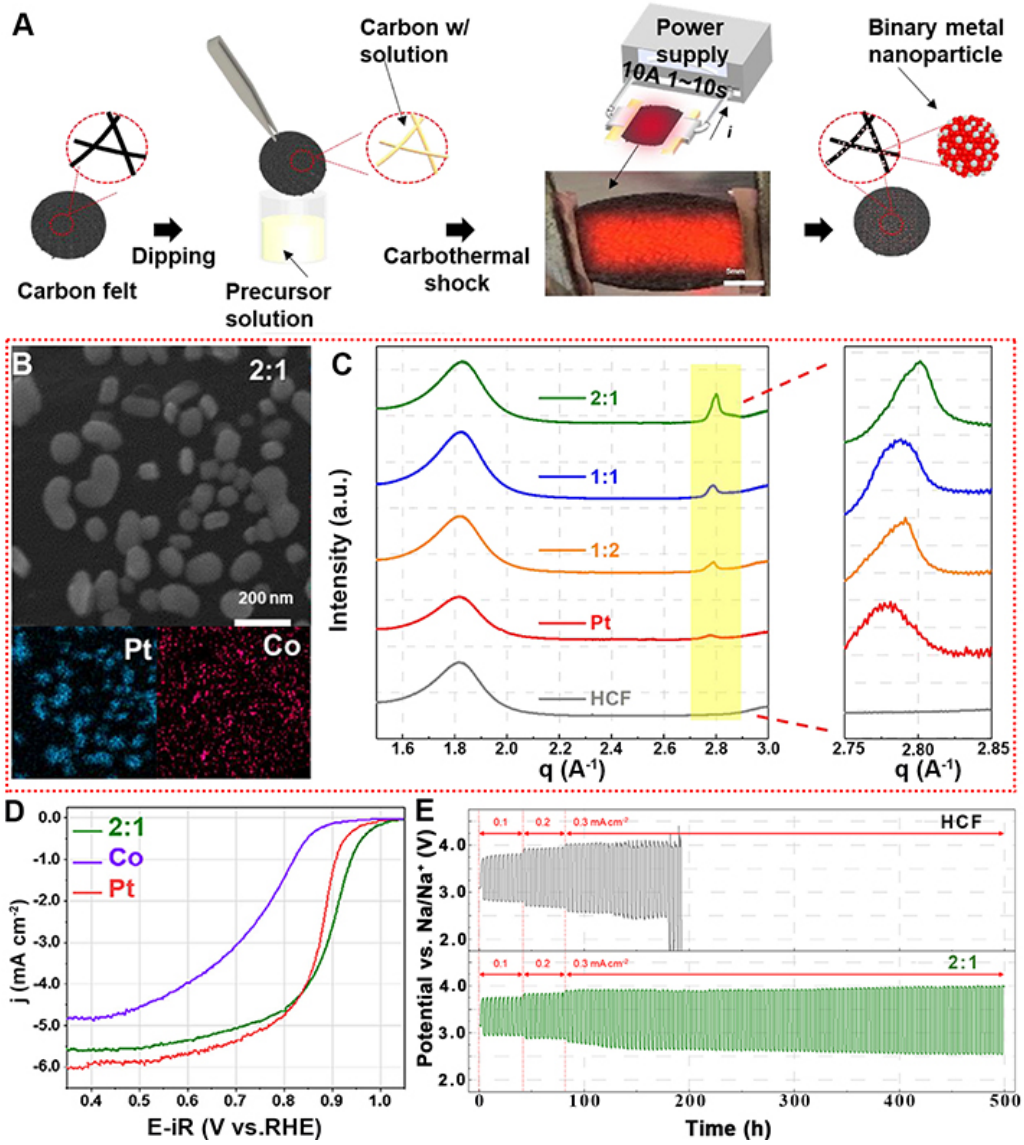

Figure 4. (A) Schematic diagram of the synthesis of Pt-Co alloy induced by CTS. (B) SEM image and EDX elemental distribution of Pt and Co in Pt-Co alloys (Pt:Co = 2:1). (C) Grazing incidence X-ray diffraction (GIXD) patterns of HCF, Pt, and Pt-Co alloys with different ratios. (D) ORR performance of the corresponding samples tested in 1.0 M KOH solutions. (E) Galvanostatic charge/discharge curves of seawater batteries with/without Pt-Co alloys on HCF at different current densities. (Reproduced with permission[91]. Copyright 2021, Elsevier).

In general, although the chlorine resistance of noble metal-based catalysts is enhanced and the ORR performance in seawater is improved, the relatively high charging potential and the low power density of the as-developed seawater battery deny its inherent advantages. Therefore, numerous studies have been devoted to the development of non-noble metals or metal-free ORR electrocatalysts as alternatives.

Non-noble metal-based ORR electrocatalysts

With advantages such as low cost, excellent corrosion resistance, high conductivity, high surface area, and good mechanical properties, TM-based electrocatalysts were highly developed as the cathode materials for being utilized in SMABs[93-96]. Particularly noteworthy is the design and synthesis of the TM composites with functional carbon materials to tune the intrinsic activity and stability of active sites. In the composited

structure, TMs can increase the degree of graphitization of carbon materials during carbonization. At the same time, encapsulating carbon materials on the surface of metal sites can effectively prevent metal agglomeration and promote electron transfer. Suh *et al.* designed a graphene-nanotube-cobalt hybrid electrocatalyst (S-rGO-CNT-Co) as a highly active seawater cathode catalyst [Figure 5A][97]. The reported S-rGO-CNT-Co is composed of tubular CNTs and partially anchored 10-30 nm Co NPs [Figure 5B]. The composite nanostructure of the Co-C and graphene protective layer prevents the adsorption of Cl^- on the cobalt and enhances the catalytic activity and stability of ORR. The S-rGO-CNT-Co sample was used as an electrocatalyst for the air cathode for SMABs. At a current density of 0.01 mA cm^{-2}, the charging voltage was 3.42 V, and the discharge voltage was 3.0 V. [Figure 5C]. Although the as-prepared electrocatalysts exhibit excellent performance, the discharge performance is still lower than that of 20 wt% Pt/C catalysts in SMABs [Figure 5D]. S-rGO-CNT-Co degraded rapidly in SMABs, even at a low current, and the cathode catalyst still suffered rapid Cl^- corrosion. Therefore, it is necessary to further modify the graphene-coated cobalt catalysts to improve their catalytic activity and stability in seawater electrolytes.

Wu *et al.* have developed a three-step method to construct defect-rich Fe-doped Co NPs coated by N-doped hierarchical carbon (D-FeCo@NHC) [Figure 6A][98]. The as-prepared D-FeCo@NHC has a typical core-shell structure with metal NPs encapsulated in carbon, which can promote the electrical conductivity and corrosion resistance of catalysts [Figure 6B]. Besides, Fe doping can not only promote the formation of metal defects but also adjust the electronic structure of D-FeCo@NHC. Meanwhile, DFT theoretical calculations show that the combination of metal and carbon defect synergistically optimized the d-band center of the sample and thus boosted the ORR activity [Figure 6C]. As shown in Figure 6D and E, the D-FeCo@NHC exhibits a high $E_{1/2}$ of 0.874 V in alkaline seawater electrolytes, and the as-assembled battery shows a high peak power density and long cycling stability.

In addition, TM-based single-atom electrocatalysts have been widely employed, which show promising potential for being utilized as ORR electrocatalysts. Typically, Fe-N moieties on carbon matrix (Fe-N-C) catalysts show excellent ORR activity in alkaline and acidic electrolytes. Furthermore, compared with Pt/C and other noble metal-based catalysts, the Fe-N-C catalysts generally show excellent resistance to chlorine poisoning. Based on the mentioned above, Fe-N-C catalysts have the potential as cathode materials in the SMABs. However, up to now, little attention has been paid to its practical application in real seawater environments. Gao *et al.* reported a microwave heating method and synthesized the atomically dispersed Fe-N-G/CNT catalyst in a short time, which possesses high activity and a strong oxygen-philic interface between graphene and CNTs [Figure 7A][99]. In addition, DFT calculations and experimental results indicate that the high oxygen affinity of the catalyst is caused by the double adsorption sites on the G/CNT interface, and the high activity of Fe-N_4 active sites is due to charge separation [Figure 7B-E]. The Fe-N-G/CNT shows an excellent ORR performance in both O_2-saturated alkaline solution and seawater with $E_{1/2}$ of 0.929 and 0.704 V, respectively, which are much better than commercial Pt/C [Figure 7F]. In addition, the SMAB with Fe-N-G/CNT as the cathode exhibits good battery performance in oxygen-poor seawater (≈ 0.4 mg L^{-1}), where the discharge voltage at 10 mA cm^{-2} is 1.18 V [Figure 7G].

Although big progress has been made in the development and the application of Fe-N-C as the ORR electrocatalysts in seawater batteries, the catalytic influencing mechanism of the Cl^- resistance of Fe-N-C catalysts is still unclear and remains a challenge. Zhan *et al.* prepared an atomic electrocatalyst by anchoring Fe-N_x sites on N-doped activated carbon substrates (Fe-N_x/NAC) to explore the effect of Cl^- on Fe-N_x/NAC ORR performance[100]. The isolated single Fe atom is well dispersed and embedded on porous NAC, and the Fe, C, N, and O elements are uniformly distributed throughout the active carbon matrix [Figure 8A and B]. Benefiting from the abundance of Fe-N_x active sites, high surface area of activated carbon, and good

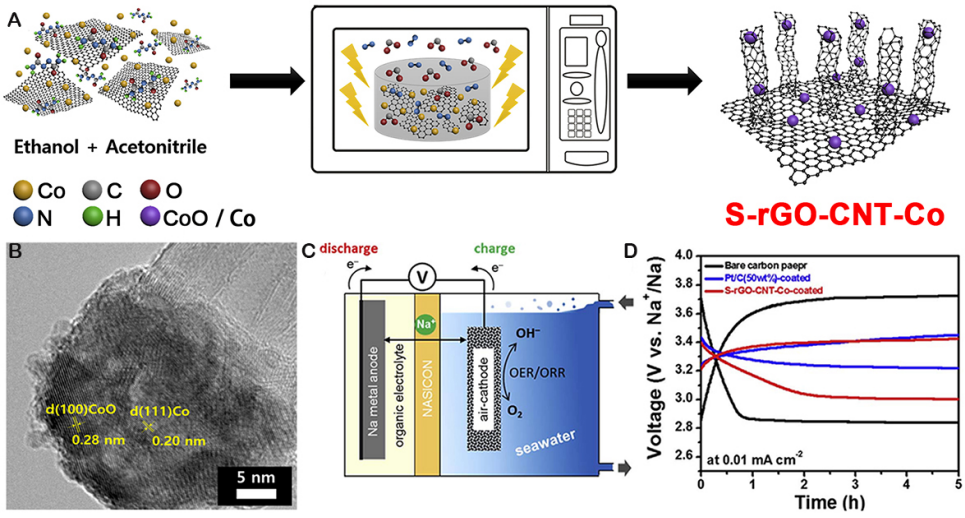

Figure 5. (A) The schematic diagram shows the microwave synthesis process of S-rGO-CNT-Co. (B) HRTEM image of the S-rGO-CNT-Co. (C) Structure diagram of seawater flow batteries. (D) The first charge-discharge voltage diagram of seawater flow batteries with different electrocatalysts. (Reproduced with permission[97]. Copyright 2017, Elsevier).

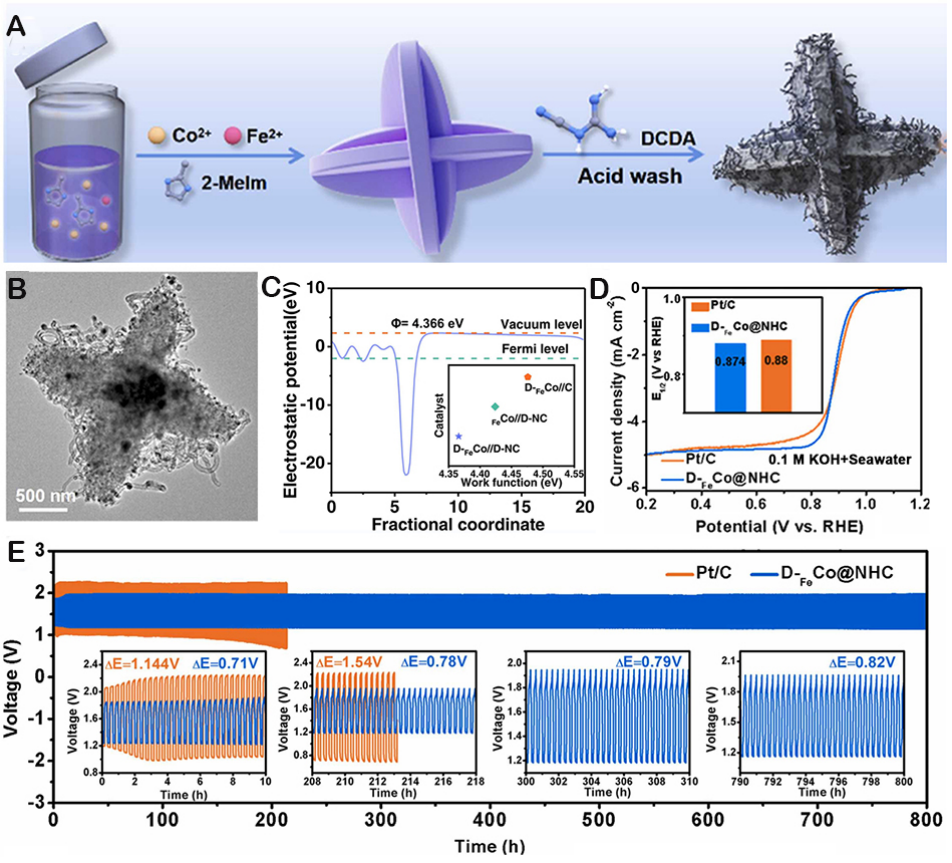

Figure 6. (A) The synthesis route diagram of D-FeCo@NHC. (B) HRTEM images of S-rGO-CNT-Co. (C) LSV curves of D-FeCo@NHC and Pt/C catalyst for ORR in 0.1 M KOH + seawater. (D) Computed work functions of D-FeCo//D-NC. (E) Galvanostatic discharge-charge cycling stability of liquid ZAB. (Reproduced with permission[98]. Copyright 2023, Elsevier).

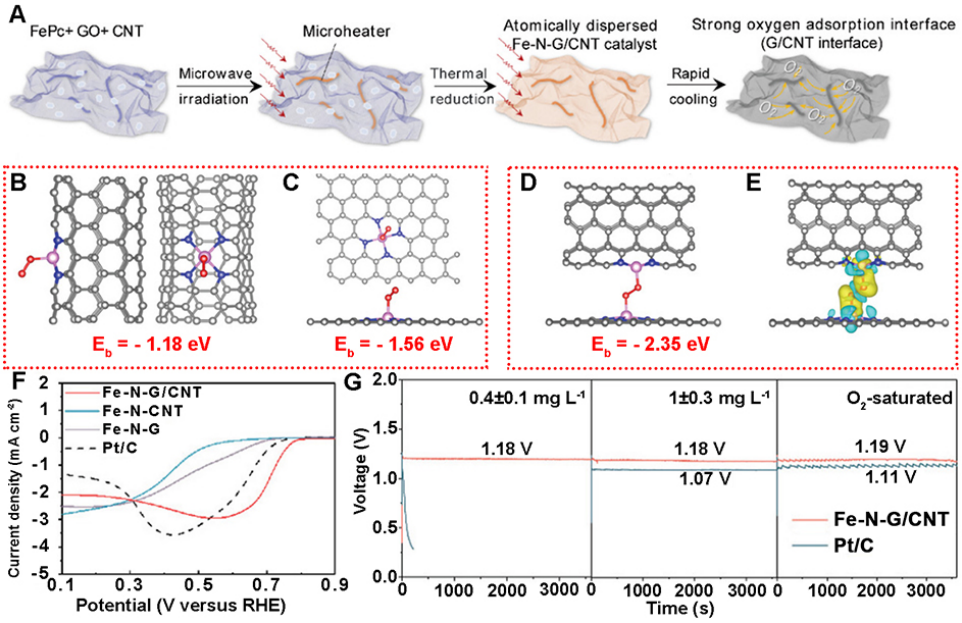

Figure 7. (A) Schematic illustration of the synthesis of Fe-N-G/CNT. (B-D) Geometry of the O_2 adsorption mechanism on (B) Fe-N-CNT; (C) Fe-N-G; and (D) Fe-N-G/CNT and the corresponding O_2 adsorption binding energies. (E) The three-dimensional charge density distribution of Fe-N-G/CNT absorbed O_2. (F) LSV curves of the corresponding electrocatalysts in O_2-saturated artificial seawater. (G) Discharge curves for different oxygen contents. (Reproduced with permission[99]. Copyright 2021, Wiley-VCH).

resistance to Cl^- adsorption, Fe-N_x/NAC exhibits good ORR catalytic activity and high stability in 3.5 wt% NaCl solution, which exceeds the performance of Pt/C. In addition, the effect of Cl^- concentration on Fe-N_x/NAC activity was also studied. As shown in Figure 8C-E, with the increase in NaCl concentration, no significant activity change was observed. For composition, Pt, NAC, and FeO_x/AC were all poisoned by the strong Cl^- adsorption. However, Fe-N_x/NAC was not affected by Cl^- adsorption to some extent, and the ORR activity can remain stable. Moreover, to investigate the Cl^- poisoning resistance of Fe-N_x and Pt (111) sites, the reaction-free energies of OH^- and Cl^- desorption were calculated, respectively. The adsorption sites of the pyrrole(C) of Fe-N_4/NAC are demonstrated in Figure 8F by the structures of OH^- and Cl^- adsorption. As shown in Figure 8G, When the reaction Gibbs free energy, ΔGr, O_2 of O_2 adsorption were investigated, it was found that the steps strongly related to ORR activity in alkaline and neutral solutions showed that the C site was not the main reaction center of ORR. As shown in Figure 8H, The calculation was performed on Fe sites in Fe-N_x/NACs at 0 V and 0.6 V. The reaction-free energy of OH^- and Cl^- desorption is more positive than that on Pt (111), which indicates that the adsorption energy of anions on Fe-N_4/NAC is stronger. This corrected desorption-free energy is consistent with the fact that Fe atoms are positively charged (Fe-pyridine is +1.34, Fe-pyrrole is +1.41) and easily attract anions. On the contrary, the Pt atom on Pt (111) is almost neutral (-0.04), so it is less attractive to anions. Although the Fe reaction center was blocked, the Fe-pyrroline-C site remained unblocked due to the discovery that Cl^- could not be bonded to the carbon atom of the electrocatalysts.

TM oxides also show promising ORR catalytic activity in seawater conditions[101]. Kim *et al.* developed cobalt manganese oxide (CMO) as cathode electrocatalysts for rechargeable seawater batteries[84].The porous CMO NPs exhibit good bifunctional electrocatalytic activities for the ORR and OER processes, with stable cycle performance and high round-trip efficiencies (up to 85% at a current density of 0.01 mA cm^{-2}). In addition, with a hard carbon electrode as the anode and the CMO as the electrocatalyst, the Na-free seawater batteries display excellent cycle performance. After 100 cycles, the average discharge voltage is

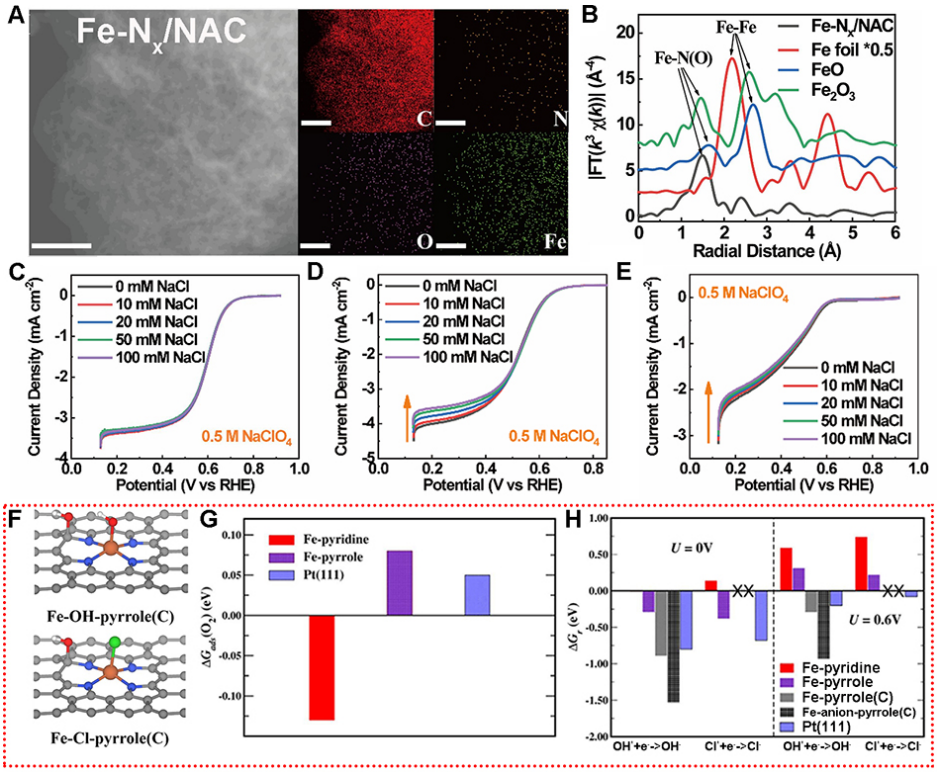

Figure 8. (A) The element maps and (B) Fe K-edge XANES spectra of Fe-N_x/NAC. LSV polarization curves of (C) Fe-N_x/NAC, (D) NAC, and (E) FeO_x/AC in 0.5 M $NaClO_4$ with different NaCl concentrations at 1,600 rpm. (F) The structure of Fe-N_4/NAC adsorbing O_2, OH^-, and Cl^- calculated by DFT (H: white; O: red; Cl: green). (G) DFT calculation results of adsorption free energy of O_2 on Pt (111) and Fe-N_4/NAC. (H) The reaction-free energies of Cl^- desorption and OH^- desorption from Pt (111) phase and Fe-N_4/NAC at $\alpha(Cl^-)$ = 0.5 mol L^{-1} and pH = 7. (Reproduced with permission[100]. Copyright 2022, Elsevier).

≤2.7 V, the coulombic efficiency is as high as 96%, and the energy efficiency is up to 74%-79%. Moreover, Son *et al.* fabricated a sacrificial electrocatalyst with Pt NP-modified 1T-MoS_2 layers by a CTS strategy [Figure 9A][102]. The HRTEM image clearly shows that the Pt NPs are uniformly anchored on the MoS_2 layer [Figure 9B]. Furthermore, the deconvolution region of the Pt 4f and Mo 3d XPS spectra show that electron transfer from Pt to MoS_2 layers, which increased the proportion of the 1T-MoS_2 phase in CTS-Pt@MoS_2 than that in CTS-MoS_2 [Figure 9C and D]. Besides, compared to those of the CTS-MoS_2 electrode, the introduction of Pt NPs improves the ORR activity of the CTS-MoS_2 electrode during the discharge process and further reduces the potential [Figure 9E]. The CTS-Pt@MoS_2 catalyst significantly improves the electrochemical performance of the fabricated seawater battery, achieving a high-power density of 6.56 mW cm^{-2}, a low discharge/charge potential gap of Δ0.39 V, and excellent long-term cycle stability of up to 400 h at a low charge potential (3.39-3.6 V) [Figure 9F]. Due to slight oxidation of the edges of the MoS_2 layer after 450 h of cycling, there is an increase in the voltage gap during charging and discharging. However, it can still work for at least 350 h at 4.0-2.6 V.

Metal-free ORR electrocatalysts

The study of metal-free catalysts, especially N-doped functional carbon materials, has attracted more attention for their application in seawater batteries. Zhang *et al.* fabricated a three-dimensional (3D) microporous carbon sponge by the simple pyrolysis of the formaldehyde-melamine-sodium bisulfite copolymer, which shows superior electrocatalytic activity and stability[103]. The excellent electrocatalytic performance can be attributed to the following three parts. Firstly, the as-prepared 3D macroporous carbon

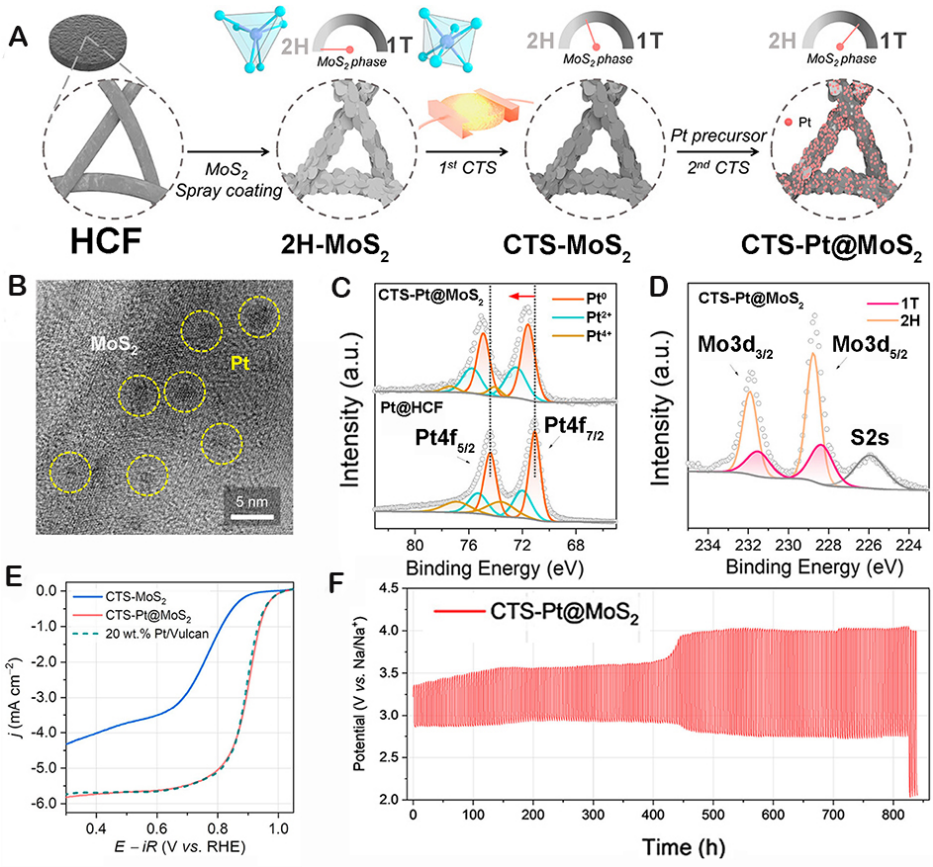

Figure 9. (A) Synthesis schematic of the Pt nanoparticle-modified 1T-MoS_2 sacrificial catalyst (1T: trigonal antiprismatic phase; 2H: hexagonal prismatic phase). (B) HRTEM image of CTS-Pt@MoS_2. (C) Pt 4f XPS profiles of pristine Pt@HCF and CTS-Pt@MoS_2. (D) Mo 3d XPS profiles of CTS-Pt@MoS_2. (E) LSV curves for determining the ORR activities of CTS-MoS_2, CTS-Pt@MoS_2, and 20 wt% Pt/Vulcan electrodes. (F) Galvanostatic charge/discharge cycling behavior of the CTS-Pt@MoS_2 electrode. (Reproduced with permission[102]. Copyright 2022, American Chemical Society).

sponge exhibits excellent electrocatalytic activity toward the OER/ORR in seawater. The fabricated hybrid sodium-seawater flow battery prepared with a 3D macroporous carbon sponge as the cathode exhibits excellent battery behavior, high discharging voltage and energy efficiency, excellent rechargeability, and long-term cycle stability. The incorporation of nitrogen- and oxygen-containing groups in carbon skeletons and the defective structure provide abundant electrocatalytic active sites for OER/ORR. Secondly, the microporous structure provides a large number of pathways for the efficient transportation of dissolved O_2, OH^-, and H_2O, which greatly enhances the OER/ORR performance. Thirdly, graphitization and interconnected carbon scaffolds form a 3D conductive network with rapid electron transfer, which promotes electrochemical OER/ORR activity. Kha Tu *et al.* prepared a controllable N-doped high specific surface area carbon cloth by a simple thermal annealing process [Figure 10A][104]. The N-doped carbon cloth prepared at 700 °C contains a high density of pyridinic-nitrogen sites, which is beneficial to improving the ORR and OER activity [Figure 10B]. At a current density of 0.25 mA cm^{-2}, the pyridinic-nitrogen-dominated carbon cathode exhibits excellent SMAB performance, such as a low overpotential gap of 0.84 V and high-power density of 9.66 mW cm^{-2} [Figure 10C]. Moreover, the ORR active sites of the N-doped carbon cloth were confirmed to be related to the adjacent carbon atoms of pyridinic-nitrogen located at the zigzag edge of the carbon structure or single vacancy defect [Figure 10D and E].

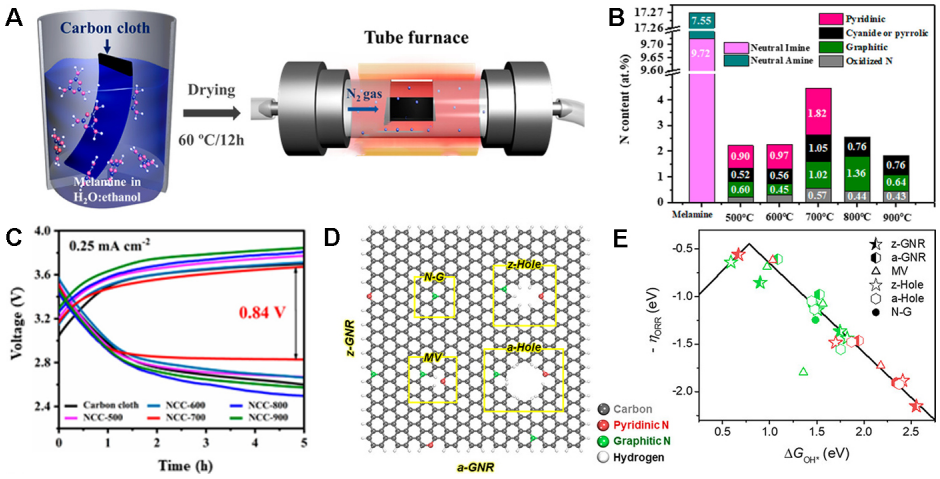

Figure 10. (A) Schematic illustration of the preparation of carbon cloths (CCs). (B) The type of nitrogen functional groups and atomic content in the melamine attached CC and N-doped CCs with increasing annealing temperature. (C) Constant current charge-discharge voltage curves. (D) Schematic presentation of N-doped configurations. zigzag (z-GNR), armchair (a-GNR) graphene nanoribbon; N-G: graphite nitrogen-substituted graphene base surface; MV: monovacancy defect; z-Hole: zigzag-terminated hole defect; a-Hole: armchair-terminated hole defect. (E) The ORR volcano plot for the active sites mentioned above as a function of the Gibbs formation energy of the OH^* intermediate from water (ΔG_{OH^*}). (Reproduced with permission[104]. Copyright 2020, American Chemical Society).

Generally, most of the current commercial electrocatalysts are noble metal-based, such as Pt- and Ru-based electrocatalysts, which are considered as the best electrocatalysts for the ORR catalysis in seawater electrolytes. However, the high cost and scarcity of noble metals hinder their widespread and large-scale applications. Developing non-noble metal-based or metal-free electrocatalysts is a preferred strategy to avoid Cl^- toxicity inhibition behavior. Generally, the ORR electrocatalysts should meet the requirements: (i) High active site exposure and intrinsic activity to achieve high onset potential and discharge current density toward ORR; (ii) Large surface area and enough porous structures are beneficial to effective mass transfer rates and enhanced electrocatalytic kinetics; (iii) A robust chemical and mechanical stability architecture for high durability in seawater conditions; and (iv) High mass and volume activity, and finally, abundant resources at low cost.

OER ELECTROCATALYSTS IN SEAWATER ELECTROLYTE

One of the biggest challenges for OER processes in seawater-based electrolytes is the competition from the oxidation of Cl^-, including the hypochlorite formation reaction (HCFR) in an alkaline medium or the ClER in an acidic medium, which seriously affects the selectivity of electrocatalysts for OER[105,106]. Furthermore, the absorbed Cl^- anions and the possible hypochlorite/chlorine byproducts could corrode the active sites of catalysts, and the resulting hydroxy-chloride could corrode and poison the metal active sites by means of coordination dissolution[107,108]. Therefore, it is urgent to develop highly efficient and stable electrocatalysts for OER in seawater-based electrolytes. The outstanding OER electrocatalysts in the chlorine-containing electrolyte should be designed by the following aspects: (1) the excellent intrinsic OER catalytic activity; (2) the high electrochemical long-term stability and strong corrosion resistance to chlorides; (3) good conductivity; and (4) large active surface area and more exposed active sites. In this section, we discussed the development of OER electrocatalysts in the chlorine-containing electrolyte and the influence behavior of Cl^- toward the OER process.

Competition of chlorine oxidation in OER processes

Taking into the total concentration of Cl^- in seawater is approximately 0.54 M, Yu *et al.* plotted a simulated Pourbaix diagram of oxygen/chlorine electrochemistry in seawater to evaluate the relationship between the oxygen electrocatalytic reaction and the ClER during cycling, as shown in Figure 11[53]. During charging, Cl^- in seawater may participate in the HCFR or ClER process, generating hypochlorite or chlorine byproducts. Among all pH ranges, OER is thermodynamically preferred over HCFR and ClER. Particularly, OER electrocatalysts functioning at an overpotential of 480 mV in 0.1 M KOH solution can block the HCFR process in seawater electrolytes, although this is difficult at relatively large current densities. Moreover, the potential difference between oxygen and chlorine becomes slightly less with a reduction of the pH value (< 7.4), where HClO replaces ClO^- as the main production. When the pH value is less than 2.9, the equilibrium potential is near to but still higher than the 100 ~ 200 mV required by OER criteria. Thus, the OER process has higher selectivity and feasibility in the electrolyte with the presence of Cl^-.

The OER process would compete with the HCFR/ClER process in terms of reaction kinetics even though the OER process is thermodynamically superior to the HCFR/ClER during the charging process of SMABs[109]. This is because HCFR/ClER is a $2e^-$ oxidation reaction involving only a single intermediate, whereas OER is based on a complex $4e^-$ pathway that requires the removal of four protons and involves three intermediates. Moreover, the two reaction routes would partially share similar active sites. By the theory calculations based on assumed mechanisms, Hansen *et al.* discovered a scaling relationship between the binding energies of ClER and OER intermediates[110]. This indicates that electrocatalysts that easily bind oxygen-bound intermediates also tend to bind chloride-bound intermediates. The pH values, current density, and Cl^- content would also have significant impacts on this competition. Since HCFR cannot occur when the electrocatalysts provide a low overpotential, alkaline conditions are consequently preferable for selective OER in saltwater.

OER electrocatalysts in chlorine-containing electrolyte.

For the R-SMAB, the charging process depends on the OER catalysis on the air electrode. The four-electron reaction steps for the OER process would result in sluggish reaction kinetics, leading to large overpotentials; thus, the high charging voltage would restrain the performance of metal-air batteries in practice[108,111]. In the complex seawater-based electrolyte, the main challenge is the HCFR process, competing with OER under near-neutral or alkaline conditions, together with the consequent electrocatalyst corrosion[112,113]. Over the past decades, many OER electrocatalysts have been designed and prepared with excellent activity, selectivity, and stability in the chlorine-containing electrolyte, mainly including metal hydroxide-based electrocatalysts, TM compound-based electrocatalysts and hybrids, or compositing electrocatalysts. Furthermore, since the anode during seawater electrolysis also depends on the OER reaction, in order to comprehensively understand the impact of Cl^- on the OER reaction in seawater and the synthesis strategies for chloride-resistant OER electrocatalysts, this chapter will discuss the studies related to seawater electrolysis together.

Metal hydroxide-based electrocatalysts

Initiatively, Dionigi *et al.* established a general designing criterion for noble metal-free OER electrocatalysts, pointing out that the OER overpotential keeping smaller than 480 mV could achieve high selectivity in seawater in theory[114]. The designing criterion is the only one and the most favorable condition to avoid HCFR from the air electrodes of seawater-based metal-air batteries. As shown in Figure 12A, a NiFe-layered double hydroxide (NiFe-LDH) catalyst was prepared, and the linear sweep voltammetry (LSV) curves of OER were measured in 0.1 M KOH and 0.3 M borate buffer solution with/without the addition of 0.5 M NaCl. The OER process was more likely to occur at pH = 13 than at pH = 9.2, and the overpotential increased by 110 mV at 1 mA cm^{-2}. Furthermore, the overpotential at 10 mA cm^{-2} in pH = 13 reached 360 mV, which was not over 480 mV and satisfied the above criterion. Therefore, there were no changes for

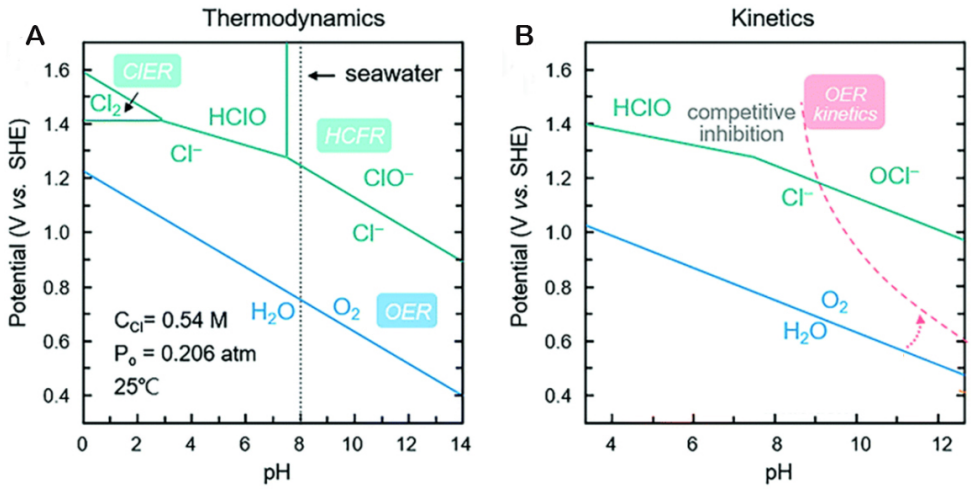

Figure 11. The Pourbaix diagram of seawater simulated according to (A) thermodynamics and (B) kinetics. (Reproduced with permission[53]. Copyright 2000, The Royal Society of Chemistry).

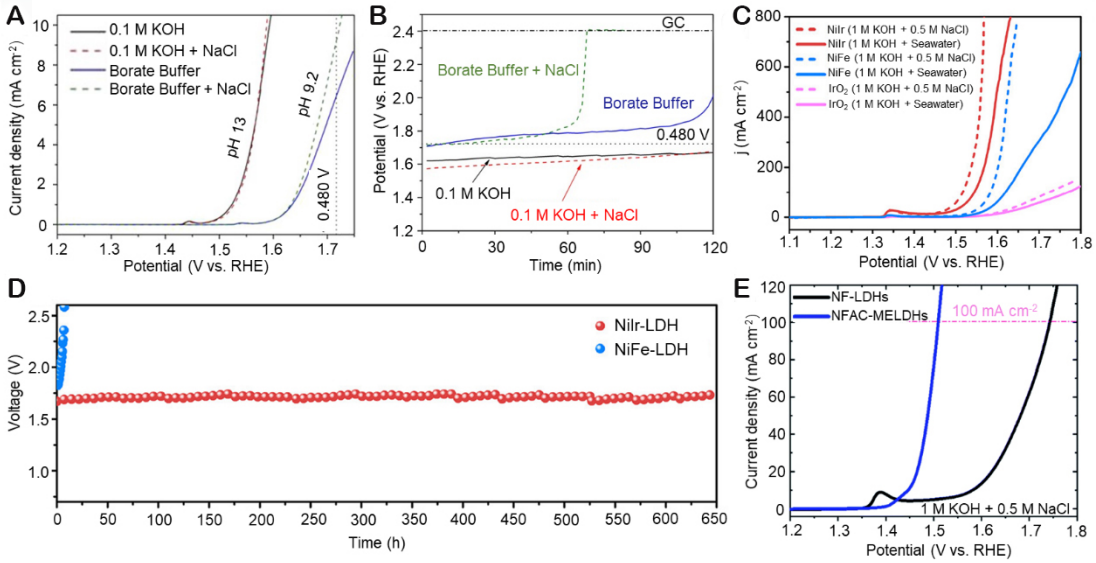

Figure 12. (A) The LSV curves of NiFe-LDH toward OER in different electrolytes. (B) Electrocatalytic stability of NiFe-LDH in different electrolytes at 10 mA cm^{-2} and 1,600 rpm. (Reproduced with permission[114]. Copyright 2016, Wiley-VCH). (C) OER LSV curves of NiIr-LDH, NiFe-LDH, and IrO_2 in two different electrolytes. (D) Durability tests of seawater catalysis (NiIr-LDH and NiFe-LDH) in 1 M KOH + seawater electrolyte at room temperature at 500 mA cm^{-2}. (Reproduced with permission[115]. Copyright 2022, American Chemical Society). (E) Seawater OER catalytic activity test for NFAC-MELDHs. (Reproduced with permission[116]. Copyright 2021, The Royal Society of Chemistry).

the overpotential with the addition of 0.5 M NaCl in 0.1 M KOH, which demonstrated the high OER selectivity. To evaluate the stability of the electrocatalysts in the electrolytes with different pH values, the NiFe-LDH catalyst was measured in the four electrolytes mentioned above by 2 h chronopotentiometry after 5 CV cycles, as shown in Figure 12B. It shows stable activity for 2 h in 0.1 M KOH, regardless of the addition of the Cl^-. Conversely, the catalytic stability of NiFe-LDH in the borate buffer became worse, especially in the presence of Cl^-. The potential rose sharply to 2.4 V after nearly 1 h at 10 mA cm^{-2} in the near-neutral chlorine-containing electrolyte, which would give rise to the undesirable HCFR process.

Therefore, moderate current density and high pH values are the key conditions for catalysts to maintain excellent electrocatalytic activity, selectivity, and long-term stability for OER processes.

Ni-based LDH electrocatalysts are known as the best OER candidates in seawater electrolytes, and NiFe LDH, in particular, is considered to be the benchmark among noble metal-free catalysts. Furthermore, in view of the considerable stability of Ir metals for OER, You *et al.* introduced Ir to develop a monolayer NiIr-LDH as an OER catalyst for seawater electrocatalysis[115]. The NiIr-LDH catalyst showed 313 mV and 361 mV overpotentials at 500 mA cm^{-2} in artificial seawater (1 M potassium hydroxide + 0.5 M NaCl) and alkaline seawater (1 M potassium hydroxide + seawater), respectively, along with nearly 100% O_2 Faradaic efficiency in alkaline seawater [Figure 12C]. Impressively, the NiIr-LDH catalyst delivered excellent long-term stability, maintaining its performance for up to 650 h under an industrial 500 mA cm^{-2} current density in alkaline seawater [Figure 12D]. Compared with the OER benchmark NiFe-LDH, both Ir and Ni are considered as the active sites for the OER in NiIr-LDH, and with the introduction of Ir, the Ni atom becomes more electrochemically active. The incorporation of Ir into the $Ni(OH)_2$ layer optimized the electron density of Ir and Ni sites and accelerated the rate-limiting step of the intermediate *O and *OOH generation on Ni and Ir sites. The synergistic effects of multi-component metallic sites are also one of the most effective strategies for constructing efficient and stable electrocatalysts in seawater conditions. Consequently, Enkhtuvshin *et al.* reported multi-metallic Ni-Fe-Al-Co-layered double hydroxides (NFAC-MELDHs) as OER catalysts (1.0 M KOH + 0.5 M NaCl), which showed an overpotential of 280 mV at a current density of 100 mA cm^{-2} [Figure 12E][116]. The Fe sites are considered to be the real active sites for redox flexibility, which cooperate with the adjacent metals to stabilize the adsorption of oxygen intermediates while promoting charge transfer.

Transition metal-based electrocatalysts

In the past decades, TM compound-based electrocatalysts have been considered as the most promising alternatives for replacing noble metal-based electrocatalysts due to their earth-abundance, popular price, potential multi-catalytic performance, and adjustable crystal and electronic structures[117-119]. Based on these advantages, strategies have been developed in recent reports to promote the OER performance of TM compound-based catalysts in seawater-based electrolytes. Accordingly, Yu *et al.* synthesized a 3D core-shell NiMoN@NiFeN OER catalyst for seawater catalysis[120]. The seawater diffusion and gas releasing processes were facilitated, benefiting from the 3D core-shell structure with multiple levels of porosity. Therefore, on the one hand, the high conductivity and large surface area of interior NiMoN nanorods led to an efficient charge transfer rate and more active sites. On the other hand, thin amorphous NiFe oxy(hydroxide) layers in situ evolved from the outer NiFeN NPs under the OER-applied voltage, acting as the active species and effectively resisting the invasion of Cl^- [Figure 13A]. The NiMoN@NiFeN catalyst showed 368 mV and 398 mV OER overpotentials at industrial current densities of 500 mA cm^{-2} and 1,000 mA cm^{-2}, respectively, in alkaline natural seawater, which are both below the 480 mV overpotential required to trigger the HCFR process [Figure 13B]. Kuang *et al.* designed a multilayer electrode NiFe/NiS_x-Ni as OER electrocatalysts in alkaline seawater [Figure 13C][121]. NiS_x was formed from the Ni foam by a solvothermal method, and NiFe hydroxide was prepared by electrodeposition using NiS_x-Ni foam as precursors. After anodic activation in an alkaline condition, the polyanion sulfate/carbonate-passivated NiFe/NiS_x-Ni foam anode was generated. After 1,000 h seawater catalysis in alkaline simulated seawater electrolyte (1 M KOH + 0.5 M NaCl), NiFe/NiS_x-Ni delivered an OER overpotential of 510 mV at the current density of 400 mA cm^{-2}, which could reach 300 mV at 400 mA cm^{-2} after iR compensation and was below the 480 mV to limited the chloride oxidation to hypochlorite [Figure 13D]. Even under the condition of high temperature (80 °C), alkalinity (6 M KOH), and salinity (1.5 M NaCl), the catalyst still shows similar excellent activity. Generally, NiFe is a highly active and selective OER catalyst for seawater electrolysis, and the interior NiS_x layer is a conductive

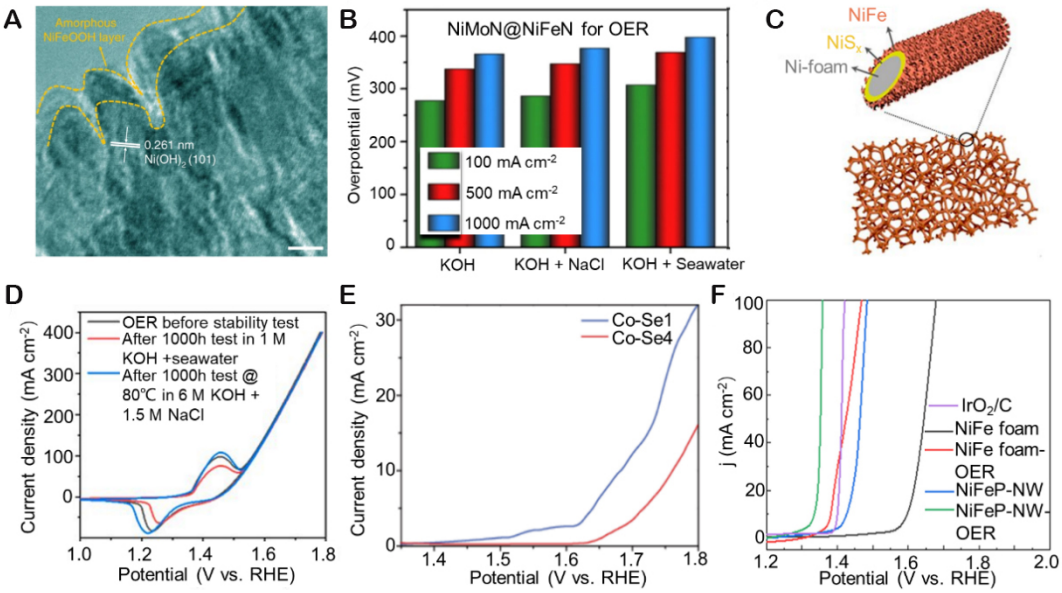

Figure 13. (A) HRTEM image of the NiMoN@NiFeN catalyst after OER tests. Scale bars: 5 nm. (B) Comparison of the OER overpotentials at 100, 500, and 1,000 mA cm^{-2} for NiMoN@NiFeN in different electrolytes. (Reproduced with permission[120]. Copyright 2019, Springer Nature). (C) Structure of the NiFe/NiS_x-Ni; (D) CV scans of a Ni^3 anode before and after 1,000 h seawater catalysis in an alkaline simulated seawater electrolyte. (Reproduced with permission[121]. Copyright 2019, PNAS). (E) The OER polarization curves of Co-Se_1 and Co-Se_4 in seawater. (Reproduced with permission[122]. Copyright 2018, WILEY-VCH). (F) OER activity of NiFe foam, NiFe foam-OER, NiFeP-NW, NiFeP-NW-OER, and IrO_2/C in alkaline simulated seawater. (Reproduced with permission[123]. Copyright 2021, Elsevier).

medium. The anion-selective polyatomic anode could effectively inhibit the corrosion by repelling Cl^-. Zhao *et al.* reported a 3D self-supporting cobalt selenide electrode by composing CoSe with Co_9Se_8 phases by regulating the Co^{3+}/Co^{2+} ratio[122]. Figure 13E shows that the combination of two cobalt selenide electrocatalysts of Co-Se_1 and Co-Se_4 with different Co ratios displays efficient OER performance in seawater electrolytes. The Co-Se_1 with a higher Co charge state reveals superior OER activity. Wang *et al.* prepared the amorphous NiFeP nanostructures as OER catalysts for overall seawater catalysis[119]. The NiFeP catalyst shows a low overpotential of 129 mV for OER at 100 mA cm^{-2} in alkaline simulated seawater electrolytes (1.0 M KOH + 0.01 M $KHCO_3$ + 1 M NaCl). The electronic states of NiFe sites are regulated by the ligand effect of the P element, which breaks the scaling relations for oxygen-containing intermediates and reduces the adsorption energy gap between HO* and HOO* from 3.08 eV to 2.62 eV [Figure 13F].

Hybrids and composite OER electrocatalysts

TM (hydr)oxides, sulfides, selenides, and phosphides have been developed to catalyze the OER process in alkaline and seawater-based electrolytes, and some of them show relatively outstanding activity and stability[123-126]. Nevertheless, single-phase electrocatalysts generally possess some disadvantages, such as poor electrical conductivity, insufficient active site exposure, *etc.* Constructing rational heterostructures has been considered as a promising approach to combine the characteristics of materials and enhance the catalytic activity via synergistic effects and electron interactions. Accordingly, Tan *et al.* developed the Ni_2Fe-LDH/$FeNi_2S_4$/NF heterostructure electrocatalyst using a partial sulfidation strategy for OER in seawater[127]. Furthermore, inspired by the perspective that sulfate layers could inhibit corrosion resistance by repelling Cl^-, 2,000 CV cycles were performed to generate the sulfate anions before measuring the OER activity of Ni_2Fe-LDH/$FeNi_2S_4$/NF [Figure 14A]. As shown in Figure 14B, Ni_2Fe-LDH/$FeNi_2S_4$/NF after CVs (post-Ni_2Fe-LDH/$FeNi_2S_4$/NF) delivered the smallest overpotentials at 50 mA cm^{-2} and 100 mA cm^{-2}, indicating its higher corrosion resistance to Cl^-. The heterostructures provide abundant hydroxide/sulfide

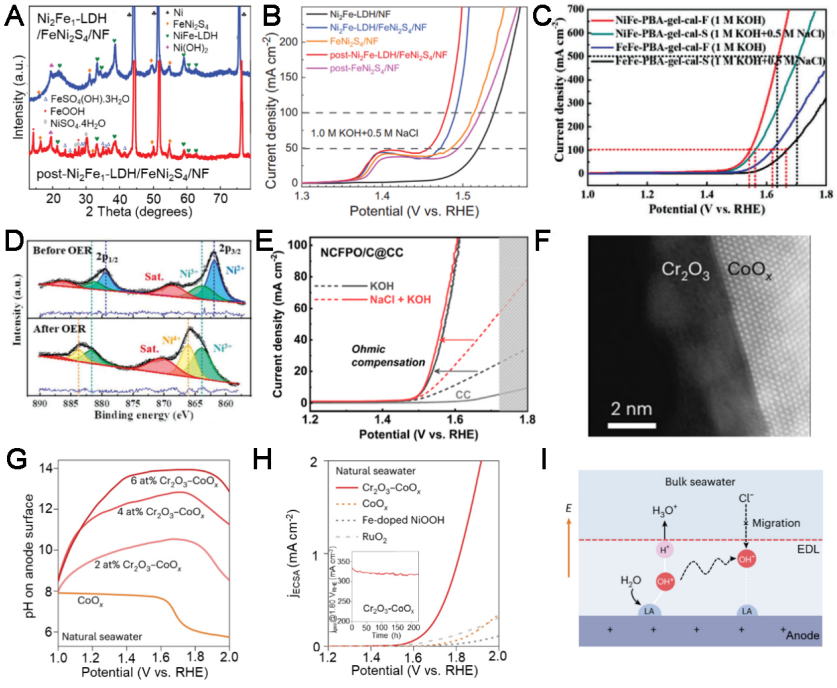

Figure 14. (A) XRD patterns of Ni_2Fe-LDH/$FeNi_2S_4$/NF and post-Ni_2Fe-LDH/$FeNi_2S_4$/NF. (B) The OER LSV curves of five different samples in 1.0 M KOH + 0.5 M NaCl. (Reproduced with permission[127]. Copyright 2022, WILEY-VCH). (C) The OER polarization curves of NiFe-PBA-gel-cal and FeFe-PBA-gel-cal in alkaline freshwater and alkaline simulated seawater. (D) The XPS spectra of Ni 2p in NiFe-PBA-gel-cal before and after OER tests. (Reproduced with permission[128]. Copyright 2022, WILEY-VCH). (E) Polarization curves of NCFPO/C@CC in the KOH and NaCl + KOH electrolytes. (Reproduced with permission[129]. Copyright 2019, American Chemical Society). (F) HAADF-STEM image of Cr_2O_3-CoO_x. (G) Measured pH values on CoO_x and Cr_2O_3-CoO_x anode surfaces at different potentials. (H) OER LSV curves of 6 at% Cr_2O_3-CoO_x, CoO_x, Fe-doped NiOOH and RuO_2 catalysts in seawater. The inset shows the durability test of the 6 at% Cr_2O_3-CoO_x anode. (I) The Schematic diagram of local alkaline microenvironment generation of Lewis acid modified anode. (Reproduced with permission[130]. Copyright 2023, Springer Nature).

interfaces and form a large number of active sites. Moreover, the excellent OER activity and stability also benefit from the large surface area, good electrical conductivity, rapid charge transfer, and mass transfer rates. To fully utilize the advantages of Ni-based and Fe-based compounds for catalyzing the OER process, Zhang *et al.* reported a TM oxide/TM carbide composite electrocatalyst with a two-step procedure[128]. A Prussian blue analog (NiFe-PBA) precursor with 2D networks was prepared by a solgel method, and the precursor was further calcined in argon and air condition to continuously prepare NiFe-PBA with ultra-large surface area, which was composed of Fe_3O_4 and NiC_x. Figure 14C shows the OER activities of the catalysts in alkaline solution (1 M KOH) and alkaline artificial seawater (1 M KOH + 0.5 M NaCl). NiFe-PBA delivered enhanced OER activities in both alkaline solution and alkaline artificial seawater, which need 308 mV and 329 mV to achieve a current density of 100 mA cm^{-2}, respectively. The characterizations after OER measurement revealed that the Fe_3O_4 NPs were coated with amorphous $NiOOH_{2-x}$ reconstructed from NiC_x, thus forming the core-shell structure. The high-valence ions and abundant oxygen defects formed along with the reconstruction process [Figure 14D]. DFT calculations and the ligand field theory uncovered that the *in-situ* generated high-valence Ni^{4+} leads to the formation of local O 2p electron holes as the electrophilic centers of the OER process. Furthermore, the OER process of NiFe-PBA follows the lattice oxygen oxidation mechanism pathway due to the existence of high valence Ni^{4+} and abundant oxygen defects, which exceeds the adsorption of oxygen-containing intermediates and is beneficial to the reaction kinetics. Song *et al.* reported the carbon-coated $Na_2Co_{1-x}Fe_xP_2O_7$ NPs (NCFPO/C NPs) as OER electrocatalysts for alkaline seawater electrolysis[129]. The NCFPO/C NPs were dip-coated on the carbon cloth for OER measurement, which delivered an overpotential of 370 mV at a current density of

100 mA cm^{-2} with the iR compensation in 0.1 M KOH + 0.5 M NaCl and showed similar LSV curves with that in 0.1 M KOH [Figure 14E]. The overpotential was less than 480 mV at 100 mA cm^{-2}, which demonstrated the high selectivity for OER electrocatalysis. No reactive chlorine species were detected after the OER test in the chlorine-containing electrolyte. Moreover, the excellent long-term stability of NCFPO/C NPs was tested by CV for 10,000 cycles and chronopotentiometry for 100 h at 10 mA cm^{-2} and 50 mA cm^{-2}.

Up to now, most seawater electrolytes contain alkaline additives for seawater catalysis. The direct natural seawater catalysis without purification and alkali addition is an important technology in the future. A novel and efficient strategy is to create a favorable local reaction microenvironment on the surface of electrocatalysts for the direct natural seawater electrocatalysis. Guo *et al.* introduced a hard Lewis acid layer on the TM oxides to manipulate the local pH values for the direct seawater electrocatalysis [Figure 14F][130]. Due to the strong ability to water dissociation, a large amount of OH^- could be in situ generated on the surface of catalysts with the increased content of hard Lewis acid Cr_2O_3. In particular, the pH value on the 6 at% Cr_2O_3-CoO_x could approach 14.0 under the applied potential of 1.60 V (*vs.* RHE), which demonstrated that it was nearly in alkaline seawater [Figure 14G]. The normalized OER activity to the electrochemical surface area of 6 at% Cr_2O_3-CoO_x was much higher than those of CoO_x and benchmark Fe-doped NiOOH and RuO_2 [Figure 14H]. Furthermore, the Cr_2O_3-CoO_x could stably catalyze the natural seawater catalysis for more than 200 h at 1.8 V *vs.* RHE, higher than the potential required to trigger chloride oxidation. Most OH^- could participate in OER processes, and some residual OH^- could interact with the positive charge on the catalyst surface to constitute a stable electrical double layer (EDL) [Figure 14I]. The enrichment of OH^- prevents the diffusion and adsorption of Cl^- to the catalyst in seawater electrolytes, thus inhibiting the chlorine redox chemistry and the corrosion of the electrode. When the Cr_2O_3-CoO_x content is 6 at%, the current density of the as-developed flow type seawater electrolyzer at 1.87 V at 60 °C meets an industrial requirement of 1.0 A cm^{-2}, and it runs stably for 100 h at 500 mA cm^{-2}.

STUDY ON METAL ELECTRODES OF SMABS

Metal anodes, such as Na, Mg, Al, and Zn, play a critical role in determining the properties of cycling life, capacity, and energy density of the SMABs. Especially in R-SMABs, mainly the odium-air batteries, where the anode is made of pure sodium or sodium alloys. During the discharge process, sodium ions are released from the negative electrode, generating electrical energy. During the charging process, sodium ions in the seawater at the negative electrode are reduced to metallic sodium. Sodium is abundantly available and is often used as anode material due to its high theoretical capacity of up to 1,166 mA g^{-1}. However, the uncontrolled growth of sodium dendrites hinders the safe operation of cells, damages the separator membrane, and shortens the device lifetime. Additionally, seawater-based sodium-air batteries still have a low coulombic efficiency and cell performance. Currently, the problem of sodium dendrites in seawater-based sodium-air batteries can be addressed through the following approaches: (i) Electrolyte optimization. By modifying the composition and concentration of the electrolyte, the formation of sodium dendrites can be reduced. Adding additives that inhibit the growth of sodium dendrites, such as polymers or ionic liquids, can effectively suppress their growth; (ii) Electrode coating. Applying a protective coating on the surface of the negative electrode can prevent the formation and growth of sodium dendrites. This coating can be a polymer or other materials that provide sufficient mechanical strength and chemical stability to prevent penetration and damage caused by dendrites; and (iii) Design optimization. By optimizing the structure and design of the battery, the formation of sodium dendrites can be minimized. For example, using porous electrode materials or nanostructures can provide more surface area and a more uniform distribution of sodium ions, reducing dendrite formation.

To investigate the growth of sodium dendrites on the surface of sodium electrodes, it is common to use *ex-situ* digital photos or SEM images to compare the changes in the surface of the negative electrode before and after reactions. For example, Kim *et al.* effectively alleviated the problem of sodium dendrite formation by designing a 1M $NaBH_4$/ether-based (glyme) electrolytes ($NaBH_4$/DEGDME and $NaBH_4$/TEGDME)[131]. For control experiments, 1.0 M $NaClO_4$ in EC/PC + 5 wt% fluoroethylene carbonate (FEC) and 1M NaOTf in glyme electrolytes (denoted as $NaClO_4$ EC/PC + 5 wt% FEC and NaOTf/TEGDME) as reference electrolytes. As shown in Figure 15. $NaClO_4$ in carbonate solvents containing + 5 wt% FEC was rapidly decomposed upon reaction with sodium to form a solid-electrolyte interphase layer. This layer exhibited inhomogeneity, which facilitated dendrite growth. Therefore, porous and dendritic surfaces of sodium metal could be observed through SEM images and digital photos. [Figure 15A-C]. Although the sodium surface cycled by NaOTf/TEGDME is smoother and less porous than that cycled by $NaClO_4$ EC/PC + 5 wt% FEC electrolytes, a wrinkled surface with uneven local thickness was obtained [Figure 15D-F]. By contrast, it is observed that $NaBH_4$-based (glyme) electrolytes had a non-dendritic dense surface morphology, which proved that $NaBH_4$/glyme can be used as an effective strategy for 'solid-electrolyte interphase layer reconstruction' on sodium metals [Figure 15G-I].

PRACTICAL APPLICATIONS

The SMABs have promising applications in various fields, such as environmental detection, channel measuring, military operations, *etc.*[132,133]. The discharging capacity of the package of SMABs can be controlled from small-scale (< 1 kWh) to medium-scale (1-10 kWh), even to large-scale (> 1 MWh) by connecting each unit pack together. For practical applications, for instance, the small-scale SMABs can be used in light buoys and detectors. Light buoys are floating devices that can be used for marking navigational channels, indicating hazards, or serving as reference points for marine activities. These buoys are designed to be easily deployed and controlled. They are often connected to a range of devices, such as lights, reflectors, and sensors, to provide visual and navigational information to vessels. The seawater battery in the light buoy can be charged by solar cells in the sunlight, thus providing more electricity to the LED lights.

The applications of medium-scale SMABs are aimed at providing electricity for various small autonomous machines, such as maritime exploration robots and drones. They are typically equipped with various sensors and cameras to monitor and search for targets in seawater, such as drifting vessels or people who have fallen overboard. These robots and drones can keep long-duration for the undersea operations using the seawater batteries. The high energy density and long lifespan of seawater batteries are being considered as ideal energy sources for maritime search and rescue robots or drones. By retrofitting and modifying existing robots or drones and integrating seawater batteries into their design, their endurance and operational efficiency can be enhanced, thereby better supporting the maritime search and rescue tusks. Moreover, there is great potential for the large-scale SMABs with energy capacities exceeding 1 MWh. These energy storage systems play a crucial role in providing electricity, stabilizing the grid, and integrating renewable energy sources into the power system. They can be utilized in various equipment, such as power plants, utility-scale renewable energy projects, industrial facilities, and large commercial buildings.

CONCLUSION AND OUTLOOK

SMABs directly utilize seawater as the electrolyte to achieve high energy density, long-term stability, and distributed, *in-situ* power supply systems, which possess broad application prospects. However, the application of OER/ORR catalysts as air cathodes is different from traditional alkaline metal-air batteries due to the influence of high content of Cl^- in seawater on the electrocatalytic processes. To improve the intrinsic OER/ORR electrocatalytic activity and stability, various electrocatalyst materials have been developed, such as noble metal-based, non-noble metal-based, and metal-free electrocatalysts. Some of these

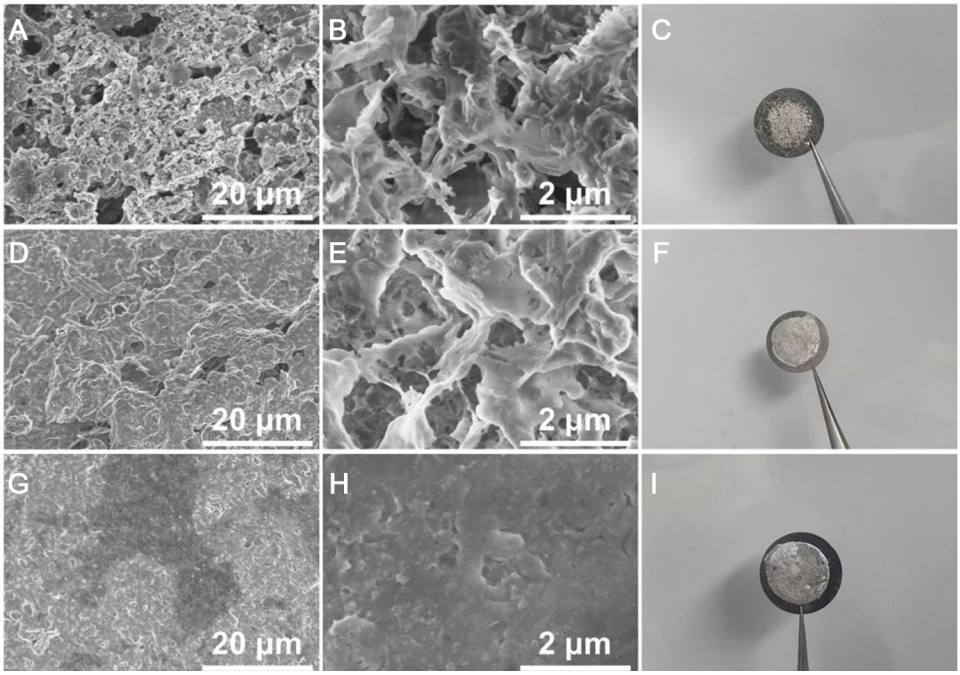

Figure 15. SEM images and digital photos for sodium metal electrodes of Na||Na symmetric cells after 50 cycles at 1 mA cm^{-2}, 1 mAh cm^{-2}. (A-C) $NaClO_4$ EC/PC + 5 wt% FEC, (D-F) NaOTf/TEGDME (G-I) $NaBH_4$/DEGDME (Reproduced with permission[131]. Copyright 2022, The Royal Society of Chemistry).

materials exhibit satisfactory OER/ORR activity, selectivity, and stability in the presence of Cl^- in seawater. As mentioned above, the intrinsic electrocatalytic ability can be improved by adjusting the electronic structure and atomic-scale surface-interface structure. It is believed that new insights into promoting the electrocatalytic processes of OER/ORR in chloride-containing and seawater electrolytes will lay the foundation for designing SMABs.

The further optimization of SMABs makes them possess promising applications as self-powering systems for the equipment working in the deep and open sea. In order to enhance the battery performance, several directions should be given more attention. Firstly, it is necessary to unveil the mechanism of CI^- corrosion in the ORR process. The combination of theoretical calculations and *in-situ* experimental investigations is required to reveal the effect of CI^- on ORR efficiency and stability. This will provide important theoretical and experimental foundations for the development of chlorine-resistant, efficient, and stable ORR/OER bifunctional oxygen electrocatalysts. Secondly, paying attention to the overall system design and integration is important to establish practical and scalable SMABs. This includes optimizing cell configurations, stack designs, and system components to maximize energy conversion efficiency and ensure long-term stability. Thirdly, more efforts should be devoted to the optimization of membranes to enhance the transfer rate of definite ions and improve the energy conversion efficiency and stability. When addressing these key issues, researchers may pave the way for the development of more efficient, stable, and environmentally friendly SMABs.

DECLARATIONS

Authors' Contributions

Conceptualization, investigation, and writing-original draft: Guo Y, Cao Y, Lu J

Writing-review & editing: Guo Y, Zheng X
Writing-review & editing, supervision, and funding acquisition: Zheng X, Deng Y

Availability of data and materials
Not applicable.

Financial support and sponsorship
This work was supported by the National Natural Science Foundation of China (52231008, 52177220) and the Key Research and Development Project of Hainan Province (ZDYF2022GXJS006).

Conflicts of interest
All authors declared that there are no conflicts of interest.

Ethical approval and consent to participate
Not applicable.

Consent for publication
Not applicable.

REFERENCES
1. Helveston JP, He G, Davidson MR. Quantifying the cost savings of global solar photovoltaic supply chains. *Nature* 2022;612:83-7. DOI PubMed
2. Russo G. Renewable energy: wind power tests the waters. *Nature* 2014;513:478-80. DOI PubMed
3. Aziz MJ, Gayme DF, Johnson K, et al. A co-design framework for wind energy integrated with storage. *Joule* 2022;6:1995-2015. DOI
4. Almora O, Baran D, Bazan GC, et al. Device performance of emerging photovoltaic materials (version 1). *Adv Energy Mater* 2021;11:2002774. DOI
5. Zhang C, Wang H, Yu H, et al. Single-atom catalysts for hydrogen generation: rational design, recent advances, and perspectives. *Adv Energy Mater* 2022;12:e2200875. DOI
6. van Cresce A, Xu K. Aqueous lithium-ion batteries. *Carbon Energy* 2021;3:721-51. DOI
7. Lopes PP, Stamenkovic VR. Past, present, and future of lead-acid batteries. *Science* 2020;369:923-4. DOI PubMed
8. Kim J, Lee E, Kim H, Johnson C, Cho J, Kim Y. Rechargeable seawater battery and its electrochemical mechanism. *ChemElectroChem* 2015;2:328-32. DOI
9. Kim Y, Lee W. Secondary seawater batteries. In: Seawater batteries. Green Energy and Technology. Singapore: Springer; 2022. pp. 91-293. DOI
10. Mozaffari S, Nateghi MR. Recent advances in solar rechargeable seawater batteries based on semiconductor photoelectrodes. *Top Curr Chem* 2022;380:28. DOI PubMed
11. Khan Z, Park SO, Yang J, et al. Binary N,S-doped carbon nanospheres from bio-inspired artificial melanosomes: a route to efficient air electrodes for seawater batteries. *J Mater Chem A* 2018;6:24459-67. DOI
12. Sun Q, Dai L, Luo T, Wang L, Liang F, Liu S. Recent advances in solid-state metal-air batteries. *Carbon Energy* 2023;5:e276. DOI
13. Li Y, Lu J. Metal-air batteries: will they be the future electrochemical energy storage device of choice? *ACS Energy Lett* 2017;2:1370-7. DOI
14. Rahman MA, Wang X, Wen C. High energy density metal-air batteries: a review. *J Electrochem Soc* 2013;160:A1759-71. DOI
15. Zhang J, Zhang J, He F, et al. Defect and doping co-engineered non-metal nanocarbon ORR electrocatalyst. *Nanomicro Lett* 2021;13:65. DOI PubMed PMC
16. Chen Y, Xu J, He P, et al. Metal-air batteries: progress and perspective. *Sci Bull* 2022;67:2449-86. DOI
17. Galili N, Shemesh A, Yam R, et al. The geologic history of seawater oxygen isotopes from marine iron oxides. *Science* 2019;365:469-73. DOI
18. Gayen P, Saha S, Ramani V. Pyrochlores for advanced oxygen electrocatalysis. *ACC Chem Res* 2022;55:2191-200. DOI PubMed
19. Lv X, Wei W, Wang H, Huang B, Dai Y. Multifunctional electrocatalyst PtM with low Pt loading and high activity towards hydrogen and oxygen electrode reactions: a computational study. *Appl Catal B* 2019;255:117743. DOI

20. Cui X, Ren P, Ma C, et al. Robust interface Ru Centers for high-performance acidic oxygen evolution. *Adv Mater* 2020;32:e1908126. DOI
21. Kwon J, Sun S, Choi S, et al. Tailored electronic structure of Ir in high entropy alloy for highly active and durable bifunctional electrocatalyst for water splitting under an acidic environment. *Adv Mater* 2023;35:e2300091. DOI
22. Cai J, Zhang H, Zhang L, Xiong Y, Ouyang T, Liu ZQ. Hetero-anionic structure activated Co-S bonds promote oxygen electrocatalytic activity for high-efficiency zinc-air batteries. *Adv Mater* 2023;35:e2303488. DOI
23. Kim C, Min H, Kim J, Moon JH. Boosting electrochemical methane conversion by oxygen evolution reactions on Fe-N-C single atom catalysts. *Energy Environ Sci* 2023;16:3158-65. DOI
24. Gao FY, Gao MR. Nickel-based anode catalysts for efficient and affordable anion-exchange membrane fuel cells. *ACC Chem Res* 2023;56:1445-57. DOI PubMed
25. Wang L, Snihirova D, Deng M, et al. Sustainable aqueous metal-air batteries: an insight into electrolyte system. *Energy Stor Mater* 2022;52:573-97. DOI
26. Zhang W, Chang J, Wang G, et al. Surface oxygenation induced strong interaction between Pd catalyst and functional support for zinc-air batteries. *Energy Environ Sci* 2022;15:1573-84. DOI
27. Kim S, Ji S, Yang H, et al. Near surface electric field enhancement: pyridinic-N rich few-layer graphene encapsulating cobalt catalysts as highly active and stable bifunctional ORR/OER catalyst for seawater batteries. *Appl Catal B* 2022;310:121361. DOI
28. Zhu J, Chi J, Cui T, et al. F doping and P vacancy engineered FeCoP nanosheets for efficient and stable seawater electrolysis at large current density. *Appl Catal B* 2023;328:122487. DOI
29. Stamenkovic V, M. Markovic N, Ross P. Structure-relationships in electrocatalysis: oxygen reduction and hydrogen oxidation reactions on Pt(111) and Pt(100) in solutions containing chloride ions. *J Electroanal Chem* 2001;500:44-51. DOI
30. Liu K, Fu J, Lin Y, et al. Insights into the activity of single-atom Fe-N-C catalysts for oxygen reduction reaction. *Nat Commun* 2022;13:2075. DOI PubMed PMC
31. An L, Hu Y, Li J, et al. Tailoring oxygen reduction reaction pathway on spinel oxides via surficial geometrical-site occupation modification driven by the oxygen evolution reaction. *Adv Mater* 2022;34:e2202874. DOI
32. Wang N, Ou P, Hung SF, et al. Strong-proton-adsorption Co-based electrocatalysts achieve active and stable neutral seawater splitting. *Adv Mater* 2023;35:e2210057. DOI
33. Hwang SM, Park JS, Kim Y, et al. Rechargeable seawater batteries-from concept to applications. *Adv Mater* 2019;31:e1804936. DOI
34. Blake IC. Fiftieth anniversary: the anniversary issue on primary cell: silver chloride-magnesium reserve battery. *J Electrochem Soc* 1952;99:202C. DOI
35. Huang Q, Yu K, Yang S, Wen L, Dai Y, Qiao X. Effects of Al and Sn on electrochemical properties of Mg-6%Al-1%Sn (mass fraction) magnesium alloy as anode in 3.5%NaCl solution. *J Cent South Univ* 2014;21:4409-14. DOI
36. Wang N, Wang R, Peng C, Peng B, Feng Y, Hu C. Discharge behaviour of Mg-Al-Pb and Mg-Al-Pb-In alloys as anodes for Mg-air battery. *Electrochim Acta* 2014;149:193-205. DOI
37. Abdulrehman T, Yousif Z, Al-ameri S, Abdulkareem I, Abdulla A, Haik Y. Enhancing the performance of Mg-Al brine water batteries using conductive polymer-PEDOT:PSS. *Renew Energ* 2015;82:125-30. DOI
38. Yu K, Xiong H, Wen L, et al. Discharge behavior and electrochemical properties of Mg-Al-Sn alloy anode for seawater activated battery. *T Nonferr Metal Soc* 2015;25:1234-40. DOI
39. Yuasa M, Huang X, Suzuki K, Mabuchi M, Chino Y. Discharge properties of Mg-Al-Mn-Ca and Mg-Al-Mn alloys as anode materials for primary magnesium-air batteries. *J Power Sources* 2015;297:449-56. DOI
40. Shi Y, Peng C, Feng Y, Wang R, Wang N. Microstructure and electrochemical corrosion behavior of extruded Mg-Al-Pb-La alloy as anode for seawater-activated battery. *Mater Des* 2017;124:24-33. DOI
41. Shi Y, Peng C, Feng Y, Wang R, Wang N. Enhancement of discharge properties of an extruded Mg-Al-Pb anode for seawater-activated battery by lanthanum addition. *J Alloys Compd* 2017;721:392-404. DOI
42. Wang L, Wang R, Feng Y, Deng M, Wang N. Effect of heat treatment on electrochemical properties of Mg-9 wt.%Al-2.5 wt.%Pb alloy in sodium chloride solution. *JOM* 2017;69:2467-70. DOI
43. Xiong H, Li L, Zhang Y, et al. Microstructure and discharge behavior of Mg-Al-Sn-in anode alloys. *J Electrochem Soc* 2017;164:A1745-54. DOI
44. Wu J, Wang R, Feng Y, Peng C. Effect of hot rolling on the microstructure and discharge properties of Mg-1.6 wt%Hg-2 wt%Ga alloy anodes. *J Alloys Compd* 2018;765:736-46. DOI
45. Li J, Chen Z, Jing J, Hou J. Electrochemical behavior of Mg-Al-Zn-Ga-In alloy as the anode for seawater-activated battery. *J Mater Sci Technol* 2020;41:33-42. DOI
46. Wu Z, Zhang H, Zou J, et al. Effect of microstructure on discharge performance of Al-0.8Sn-0.05Ga-0.9Mg-1.0Zn (wt%) alloy as anode for seawater-activated battery. *Mater Corros* 2020;71:1680-90. DOI
47. Xie Q, Ma A, Jiang J, Liu H, Saleh B. Discharge properties of ECAP processed AZ31-Ca alloys as anodes for seawater-activated battery. *J Mater Res Technol* 2021;11:1031-44. DOI
48. Huang J, Liu H, Fang H, et al. Effects of intermetallic phases on electrochemical properties of powder metallurgy Mg-6%Al-5%Pb anode alloy used for seawater activated battery. *Mater Res Express* 2022;9:066504. DOI
49. Zhao C, Liu J, Yao N, et al. Low-temperature working feasibility of zinc-air batteries with noble metal-free electrocatalysts. *Renewa* 2023;1:73-80. DOI
50. Renuka R. Influence of allotropic modifications of sulphur on the cell voltage in Mg-CuI(S) seawater activated battery. *Mater Chem*

Phys 1999;59:42-8. DOI
51. Senthilkumar ST, Go W, Han J, et al. Emergence of rechargeable seawater batteries. *J Mater Chem A* 2019;7:22803-25. DOI
52. Prasad K, Venkatakrishnan N, Mathur P. Preliminary report on the performance characteristics of the magnesium-mercurous chloride battery system. *J Power Sources* 1977;1:371-5. DOI
53. Yu J, Li B, Zhao C, Zhang Q. Seawater electrolyte-based metal-air batteries: from strategies to applications. *Energy Environ Sci* 2020;13:3253-68. DOI
54. Shinohara M, Araki E, Mochizuki M, Kanazawa T, Suyehiro K. Practical application of a sea-water battery in deep-sea basin and its performance. *J Power Sources* 2009;187:253-60. DOI
55. Liu Q, Yan Z, Wang E, Wang S, Sun G. A high-specific-energy magnesium/water battery for full-depth ocean application. *Int J Hydrog Energy* 2017;42:23045-53. DOI
56. Al-eggiely AH, Alguail AA, Gvozdenović MM, Jugović BZ, Grgur BN. Seawater zinc/polypyrrole-air cell possessing multifunctional charge-discharge characteristics. *J Solid State Electrochem* 2017;21:2769-77. DOI
57. Jiao W, Fan Y, Huang C, Sanglin. Effect of modified polyacrylonitrile-based carbon fiber on the oxygen reduction reactions in seawater batteries. *Ionics* 2018;24:285-96. DOI
58. Zhang Q, Zhou Y, Dai W, et al. Chloride ion as redox mediator in reducing charge overpotential of aprotic lithium-oxygen batteries. *Batteries Supercaps* 2021;4:232-9. DOI
59. Kim Y, Kim G, Jeong S, et al. Large-scale stationary energy storage: seawater batteries with high rate and reversible performance. *Energy Stor Mater* 2019;16:56-64. DOI
60. Kim Y, Kim H, Park S, Seo I, Kim Y. Na ion-conducting ceramic as solid electrolyte for rechargeable seawater batteries. *Electrochim Acta* 2016;191:1-7. DOI
61. Kim Y, Shin K, Jung Y, Lee W, Kim Y. Development of prismatic cells for rechargeable seawater batteries. *Adv Sustain Syst* 2022;6:2100484. DOI
62. Son M, Park S, Kim N, Angeles AT, Kim Y, Cho KH. Simultaneous energy storage and seawater desalination using rechargeable seawater battery: feasibility and future directions. *Adv Sci* 2021;8:e2101289. DOI PubMed PMC
63. Kim Y, Jung J, Yu H, et al. Sodium biphenyl as anolyte for sodium-seawater batteries. *Adv Funct Mater* 2020;30:2001249. DOI
64. Han J, Hwang SM, Go W, Senthilkumar S, Jeon D, Kim Y. Development of coin-type cell and engineering of its compartments for rechargeable seawater batteries. *J Power Sources* 2018;374:24-30. DOI
65. Xu Y, Lv H, Lu H, et al. Mg/seawater batteries driven self-powered direct seawater electrolysis systems for hydrogen production. *Nano Energy* 2022;98:107295. DOI
66. Yu J, Zhao C, Liu J, Li B, Tang C, Zhang Q. Seawater-based electrolyte for zinc-air batteries. *Green Chem Eng* 2020;1:117-23. DOI
67. Wang C, Yu Y, Niu J, et al. Recent progress of metal-air batteries - a mini review. *App Sci* 2019;9:2787. DOI
68. Zhang T, Tao Z, Chen J. Magnesium-air batteries: from principle to application. *Mater Horiz* 2014;1:196-206. DOI
69. Park S, Ligaray M, Kim Y, Chon K, Son M, Cho KH. Investigating the influence of catholyte salinity on seawater battery desalination. *Desalination* 2021;506:115018. DOI
70. Mamtani K, Jain D, Co AC, Ozkan US. Investigation of chloride poisoning resistance for nitrogen-doped carbon nanostructures as oxygen depolarized cathode catalysts in acidic media. *Catal Lett* 2017;147:2903-9. DOI
71. Kim Y, Kim J, Vaalma C, et al. Optimized hard carbon derived from starch for rechargeable seawater batteries. *Carbon* 2018;129:564-71. DOI
72. Jin Z, Li P, Meng Y, Fang Z, Xiao D, Yu G. Understanding the inter-site distance effect in single-atom catalysts for oxygen electroreduction. *Nat Catal* 2021;4:615-22. DOI
73. Millero FJ, Feistel R, Wright DG, Mcdougall TJ. The composition of standard seawater and the definition of the reference-composition salinity scale. *Deep Sea Res Part I Oceanogr Res Pap* 2008;55:50-72. DOI
74. Kim DH, Choi H, Hwang DY, et al. Reliable seawater battery anode: controlled sodium nucleation *via* deactivation of the current collector surface. *J Mater Chem A* 2018;6:19672-80. DOI
75. Liu Q, Pan Z, Wang E, An L, Sun G. Aqueous metal-air batteries: fundamentals and applications. *Energy Stor Mater* 2020;27:478-505. DOI
76. Kim D, Park J, Lee W, Choi Y, Kim Y. Development of rechargeable seawater battery module. *J Electrochem Soc* 2022;169:040508. DOI
77. Arnold S, Wang L, Presser V. Dual-Use of seawater batteries for energy storage and water desalination. *Small* 2022;18:e2107913. DOI PubMed
78. Kim K, Hwang SM, Park J, Han J, Kim J, Kim Y. Highly improved voltage efficiency of seawater battery by use of chloride ion capturing electrode. *J Power Sources* 2016;313:46-50. DOI
79. Jung J, Hwang DY, Kristanto I, Kwak SK, Kang SJ. Deterministic growth of a sodium metal anode on a pre-patterned current collector for highly rechargeable seawater batteries. *J Mater Chem A* 2019;7:9773-81. DOI
80. Lee C, Jeon D, Park J, et al. Tetraruthenium polyoxometalate as an atom-efficient bifunctional oxygen evolution reaction/oxygen reduction reaction catalyst and its application in seawater batteries. *ACS Appl Mater Interfaces* 2020;12:32689-97. DOI
81. Kim J, Park J, Lee J, Lim W, Jo C, Lee J. Biomass-derived P, N self-doped hard carbon as bifunctional oxygen electrocatalyst and anode material for seawater batteries. *Adv Funct Mater* 2021;31:2010882. DOI
82. Kim J, Mueller F, Kim H, et al. Rechargeable-hybrid-seawater fuel cell. *NPG Asia Mater* 2014;6:e144. DOI

83. Manikandan P, Kishor K, Han J, Kim Y. Advanced perspective on the synchronized bifunctional activities of P2-type materials to implement an interconnected voltage profile for seawater batteries. *J Mater Chem A* 2018;6:11012-21. DOI
84. Kim S, Yang H, Jeong S, et al. Negative surface charge-mediated Fe Quantum dots with N-doped graphene/$Ti_3C_2T_x$ MXene as chlorine-resistance electrocatalysts for high performance seawater-based Al-air batteries. *J Power Sources* 2023;566:232923. DOI
85. Le Z, Li W, Dang Q, et al. A high-power seawater battery working in a wide temperature range enabled by an ultra-stable Prussian blue analogue cathode. *J Mater Chem A* 2021;9:8685-91. DOI
86. Guo Y, Yang M, Xie RC, Compton RG. The oxygen reduction reaction at silver electrodes in high chloride media and the implications for silver nanoparticle toxicity. *Chem Sci* 2020;12:397-406. DOI PubMed PMC
87. Hasvold Ø, Henriksen H, Melv‡r E, et al. Sea-water battery for subsea control systems. *J Power Sources* 1997;65:253-61. DOI
88. Li J, Wang N, Liu K, Duan J, Hou B. Efficient electrocatalytic H_2O_2 production in simulated seawater on ZnO/reduced graphene oxide nanocomposite. *Colloids Surf A Physicochem Eng Asp* 2023;668:131446. DOI
89. Shao M, Chang Q, Dodelet JP, Chenitz R. Recent advances in electrocatalysts for oxygen reduction reaction. *Chem Rev* 2016;116:3594-657. DOI PubMed
90. Nie Y, Li L, Wei Z. Recent advancements in Pt and Pt-free catalysts for oxygen reduction reaction. *Chem Soc Rev* 2015;44:2168-201. DOI
91. Ryu JH, Park J, Park J, et al. Carbothermal shock-induced bifunctional Pt-Co alloy electrocatalysts for high-performance seawater batteries. *Energy Stor Mater* 2022;45:281-90. DOI
92. Jin C, Nagaiah TC, Xia W, Bron M, Schuhmann W, Muhler M. Polythiophene-assisted vapor phase synthesis of carbon nanotube-supported rhodium sulfide as oxygen reduction catalyst for HCl electrolysis. *ChemSusChem* 2011;4:927-30. DOI PubMed
93. Chen Y, Matanovic I, Weiler E, Atanassov P, Artyushkova K. Mechanism of oxygen reduction reaction on transition metal-nitrogen-carbon catalysts: establishing the role of nitrogen-containing active sites. *ACS Appl Energy Mater* 2018;1:5948-53. DOI
94. Gu W, Hu L, Li J, Wang E. Recent advancements in transition metal-nitrogen-carbon catalysts for oxygen reduction reaction. *Electroanalysis* 2018;30:1217-28. DOI
95. Zhao C, Ren D, Wang J, et al. Regeneration of single-atom catalysts deactivated under acid oxygen reduction reaction conditions. *J Energy Chem* 2022;73:478-84. DOI
96. Liu M, Li N, Cao S, et al. A "pre-constrained metal twins" strategy to prepare efficient dual-metal-atom catalysts for cooperative oxygen electrocatalysis. *Adv Mater* 2022;34:e2107421. DOI
97. Suh DH, Park SK, Nakhanivej P, Kim Y, Hwang SM, Park HS. Hierarchically structured graphene-carbon nanotube-cobalt hybrid electrocatalyst for seawater battery. *J Power Sources* 2017;372:31-7. DOI
98. Wu S, Liu X, Mao H, et al. Realizing high-efficient oxygen reduction reaction in alkaline seawater by tailoring defect-rich hierarchical heterogeneous assemblies. *Appl Catal B* 2023;330:122634. DOI
99. Gao Z, Yang Q, Qiu P, et al. p-type plastic inorganic thermoelectric materials. *Adv Energy Mater* 2021;11:2100883. DOI
100. Zhan Y, Ding Z, He F, et al. Active site switching of Fe-N-C as a chloride-poisoning resistant catalyst for efficient oxygen reduction in seawater-based electrolyte. *Chem Eng J* 2022;443:136456. DOI
101. Li H, Kelly S, Guevarra D, et al. Analysis of the limitations in the oxygen reduction activity of transition metal oxide surfaces. *Nat Catal* 2021;4:463-8. DOI
102. Son M, Park J, Im E, et al. Sacrificial catalyst of carbothermal-shock-synthesized 1T-MoS_2 layers for ultralong-lifespan seawater battery. *Nano Lett* 2023;23:344-52. DOI
103. Zhang Y, Park J, Senthilkumar ST, Kim Y. A novel rechargeable hybrid Na-seawater flow battery using bifunctional electrocatalytic carbon sponge as cathode current collector. *J Power Sources* 2018;400:478-84. DOI
104. Tu NDK, Park SO, Park J, Kim Y, Kwak SK, Kang SJ. Pyridinic-nitrogen-containing carbon cathode: efficient electrocatalyst for seawater batteries. *ACS Appl Energy Mater* 2020;3:1602-8. DOI
105. Zhang F, Yu L, Wu L, Luo D, Ren Z. Rational design of oxygen evolution reaction catalysts for seawater electrolysis. *Trends Chem* 2021;3:485-98. DOI
106. Dresp S, Dionigi F, Klingenhof M, Strasser P. Direct electrolytic splitting of seawater: opportunities and challenges. *ACS Energy Lett* 2019;4:933-42. DOI
107. Vos JG, Wezendonk TA, Jeremiasse AW, Koper MTM. MnO_x/IrO_x as selective oxygen evolution electrocatalyst in acidic chloride solution. *J Am Chem Soc* 2018;140:10270-81. DOI PubMed PMC
108. Kim S, Lee T, Han S, Lee C, Kim C, Yoon J. $Ir_{0.11}Fe_{0.25}O_{0.64}$ as a highly efficient electrode for electrochlorination in dilute chloride solutions. *J Ind Eng Chem* 2021;102:155-62. DOI
109. Kim Y, Harzandi AM, Lee J, Choi Y, Kim Y. Design of large-scale rectangular cells for rechargeable seawater batteries. *Adv Sustain Syst* 2021;5:2000106. DOI
110. Hansen HA, Man IC, Studt F, Abild-Pedersen F, Bligaard T, Rossmeisl J. Electrochemical chlorine evolution at rutile oxide (110) surfaces. *Phys Chem Chem Phys* 2010;12:283-90. DOI PubMed
111. Komiya H, Shinagawa T, Takanabe K. Electrolyte engineering for oxygen evolution reaction over non-noble metal electrodes achieving high current density in the presence of chloride ion. *ChemSusChem* 2022;15:e202201088. DOI PubMed PMC
112. Zhao X, Wang Y, Shi Y, et al. Exploiting interfacial Cl^-/Cl^0 redox for a 1.8-V voltage plateau aqueous electrochemical capacitor. *ACS Energy Lett* 2021;6:1134-40. DOI
113. Vos JG, Liu Z, Speck FD, et al. Selectivity trends between oxygen evolution and chlorine evolution on iridium-based double

perovskites in acidic media. *ACS Catal* 2019;9:8561-74. DOI

114. Dionigi F, Reier T, Pawolek Z, Gliech M, Strasser P. Design criteria, operating conditions, and nickel-iron hydroxide catalyst materials for selective seawater electrolysis. *ChemSusChem* 2016;9:962-72. DOI PubMed
115. You H, Wu D, Si D, et al. Monolayer NiIr-layered double hydroxide as a long-lived efficient oxygen evolution catalyst for seawater splitting. *J Am Chem Soc* 2022;144:9254-63. DOI
116. Enkhtuvshin E, Kim KM, Kim Y, et al. Stabilizing oxygen intermediates on redox-flexible active sites in multimetallic Ni-Fe-Al-Co layered double hydroxide anodes for excellent alkaline and seawater electrolysis. *J Mater Chem A* 2021;9:27332-46. DOI
117. Zhang K, Zou R. Advanced transition metal-based OER electrocatalysts: current status, opportunities, and challenges. *Small* 2021;17:e2100129. DOI PubMed
118. Ibrahim KB, Tsai M, Chala SA, et al. A review of transition metal-based bifunctional oxygen electrocatalysts. *J Chin Chem Soc* 2019;66:829-65. DOI
119. Wang J, Zhao C, Liu J, et al. Composing atomic transition metal sites for high-performance bifunctional oxygen electrocatalysis in rechargeable zinc-air batteries. *Particuology* 2023;77:146-52. DOI
120. Yu L, Zhu Q, Song S, et al. Non-noble metal-nitride based electrocatalysts for high-performance alkaline seawater electrolysis. *Nat Commun* 2019;10:5106. DOI PubMed PMC
121. Kuang Y, Kenney MJ, Meng Y, et al. Solar-driven, highly sustained splitting of seawater into hydrogen and oxygen fuels. *Proc Natl Acad Sci USA* 2019;116:6624-9. DOI PubMed PMC
122. Zhao Y, Jin B, Zheng Y, Jin H, Jiao Y, Qiao S. Charge state manipulation of cobalt selenide catalyst for overall seawater electrolysis. *Adv Energy Mater* 2018;8:1801926. DOI
123. Liu J, Liu X, Shi H, et al. Breaking the scaling relations of oxygen evolution reaction on amorphous NiFeP nanostructures with enhanced activity for overall seawater splitting. *Appl Catal B* 2022;302:120862. DOI
124. Song Y, Xu B, Liao T, Guo J, Wu Y, Sun Z. Electronic structure tuning of 2D metal (Hydr)oxides nanosheets for electrocatalysis. *Small* 2021;17:e2002240. DOI PubMed
125. Joo J, Kim T, Lee J, Choi SI, Lee K. Morphology-controlled metal sulfides and phosphides for electrochemical water splitting. *Adv Mater* 2019;31:e1806682. DOI PubMed
126. Dutta A, Pradhan N. Developments of metal phosphides as efficient OER precatalysts. *J Phys Chem Lett* 2017;8:144-52. DOI PubMed
127. Tan L, Yu J, Wang C, et al. Partial sulfidation strategy to NiFe-LDH@$FeNi_2S_4$ heterostructure enable high-performance water/seawater oxidation. *Adv Funct Mater* 2022;32:2200951. DOI
128. Zhang H, Geng S, Ouyang M, Yadegari H, Xie F, Riley DJ. A self-reconstructed bifunctional electrocatalyst of pseudo-amorphous nickel carbide@iron oxide network for seawater splitting. *Adv Sci* 2022;9:e2200146. DOI PubMed PMC
129. Song HJ, Yoon H, Ju B, Lee D, Kim D. Electrocatalytic selective oxygen evolution of carbon-coated $Na_2Co_{1-x}Fe_xP_2O_7$ nanoparticles for alkaline seawater electrolysis. *ACS Catal* 2020;10:702-9. DOI
130. Guo J, Zheng Y, Hu Z, et al. Direct seawater electrolysis by adjusting the local reaction environment of a catalyst. *Nat Energy* 2023;8:264-72. DOI
131. Kim J, Kim J, Jeong J, et al. Designing fluorine-free electrolytes for stable sodium metal anodes and high-power seawater batteries *via* SEI reconstruction. *Energy Environ Sci* 2022;15:4109-18. DOI
132. Bae H, Park J, Senthilkumar S, Hwang SM, Kim Y. Hybrid seawater desalination-carbon capture using modified seawater battery system. *J Power Sources* 2019;410-11:99-105. DOI
133. Budde-meiwes H, Drillkens J, Lunz B, et al. A review of current automotive battery technology and future prospects. *J Aut Eng* 2013;227:761-76. DOI